CHAPTER 5: USER ANTENNAS

Dr. Vahraz Jamnejad
(with contributions from Paul Cramer)

5.0 INTRODUCTION

In the previous report on User Terminal Antennas (UTA's) for PASS (Chapter 6 of reference [1]), a variety of concepts were presented and discussed. Some of these concepts are presented in Figure 1 as reference. Two general categories of antennas were considered: Basic Terminal Antennas (BTA's), and Enhanced Terminal Antennas (ETA's). The ETA's employ relatively large and stationary (at least during operation) antennas, and are of more or less conventional designs. They will not be discussed here. The BTA's are more challenging and require further investigation in some detail. Specifically, there are some aspects of these antennas that need to be studied in further detail, in order to prove their feasibility and functionality in a technically as well as commercially viable system.

In this report we first tackle some issues that are of interest in the PASS antenna design in general. We discuss the effects of change in frequency on the size and gain requirements of the spacecraft as well as the ground antenna.

We then concentrate on the user antenna design considerations, specifically the basic terminal antennas (BTA's). We start with the fact that regardless of the specific design, the antenna has to operate at two relatively far apart frequencies, namely at 30 GHz transmit and 20 GHz receive frequencies. The challenges associated with this operation will be presented and some ways to resolve them will be presented. Then, trade-off study results will be given that provide limits on the gain, size, and complexity requirements of basic terminal antennas. Some design data and typical patterns will then be provided.

An issue that requires particular consideration is the significance of gain and figure of merit (G/T) in the transmit and receive modes of the antenna, respectively. This issue is particularly important in the light of experience gained during the mobile antenna experiments, where the increased noise temperature due to the antenna distribution network losses became a major cause of concern. This issue will be discussed at some length.

An important issue that requires particular attention is the radiation safety hazards associated with the operation of the basic personal antennas in Ka band frequencies at close range. The results of a preliminary investigation of this problem will be presented.

Finally, an outline of the critical technologies and development goals will then be presented, followed by an experimentation plan.

5.1 IMPACT OF FREQUENCY CHANGE ON USER AND SPACECRAFT ANTENNA GAIN AND SIZE

In this section we consider the effect of frequency change on gain and dimensions of the user terminal antennas of PASS. A summary of the relevant facts and figures is provided here, which is particularly useful for system designers.

The transmit antenna has a gain of

$$G_t = (4\pi / \lambda^2) A_t \tag{1}$$

in which λ is the wavelength and is related to frequency as

$$\lambda = C / f, \; C = 2.997925 \times 10^8 \text{ meters/second} \tag{2-a}$$

or

$$\lambda(\text{cm}) = 30 / f(\text{GHz}) \tag{2-b}$$

A_t in (1) is the effective aperture of the transmitting antenna in the direction of the receiving antenna. The isotopically radiated power at the receiving antenna location, EIRP, is given by

$$P_e = G_t P_t = (4\pi / \lambda^2) A_t P_t \tag{3}$$

in which P_t is the total power input to the transmitting antenna. The power density per unit areas (flux density), Φ, at a distance d, at the receiving antenna location is given by

$$\Phi = (P_e / 4\pi d^2) = (G_t / 4\pi d^2) P_t \tag{4}$$

The effective receiving aperture of the ground antenna in the direction of the incoming wave is defined as

$$A_r = (\lambda^2 / 4\pi) G_r \tag{5}$$

in which G_r is the gain of the receiving antenna in the direction of the incoming wave. The total received power, P_r, can therefore be written in one of the following equivalent forms:

$$P_r = A_r \Phi = \frac{A_t A_r}{d^2 \lambda^2} P_t = \frac{A_t A_r}{d^2 C^2} f^2 P_t \qquad (6\text{-a})$$

$$= \frac{G_t G_r}{(4\pi d/\lambda)^2} P_t = \frac{G_t G_r}{(4\pi d/C)^2} \frac{1}{f^2} P_t \qquad (6\text{-b})$$

$$= \frac{A_t G_r}{4\pi d^2} P_t \qquad (6\text{-c})$$

$$= \frac{G_t A_r}{4\pi d^2} P_t \qquad (6\text{-d})$$

The above equations are different versions of the well-known Friis transmission formula. In these formulas a polarization efficiency of 100% is assumed, i.e., the transmitter and receiver antenna field polarizations are perfectly matched. Otherwise a polarization efficiency factor must be included.

Although the second form (6-b) is usually used in link calculations in which the term $(4\pi d/\lambda)^2$ is referred to as the space loss, the other forms can sometimes be helpful in interpreting the relationships between transmit and receive antenna aperture size, gain, power, and frequency. For example, we can make the following observations.

Given a fixed distance between the transmitter and receiver, and a desired received power level,

i. from (6-a), for fixed transmit and receive antenna apertures, the required transmit power is inversely proportional to the square of frequency.

ii. from (6-b), for fixed transmit and receive antenna gains, the required transmit power is proportional to the square of frequency.

iii. from (6-c), for fixed transmitter aperture size and fixed receiver antenna gain, the required transmitter power is independent of frequency, while receiver antenna aperture size decreases with frequency increase.

iv. from (6-d), for fixed transmitter gain and fixed receiver aperture, the required transmit power remains independent of the frequency, while transmitter antenna aperture decreases with frequency increase.

Furthermore, it should be kept in mind that for a fixed gain the beamwidth remains constant, while for a fixed aperture size the beamwidth decreases with an increase in frequency. In general, the half-power (or 3-dB) beamwidth is approximately given as

$$BW^\circ \approx \frac{65}{D/\lambda} = \frac{65\ C}{D\ f}, \qquad (7)$$

for the aperture type antennas, in which D is the aperture dimension in the plane in which the beamwidth is considered.

The user terminal antenna in the PASS system is a medium gain antenna with a gain in the range of 15 to 25 dB, typically composed of an array of fixed gain radiating elements. These elements have fixed dimensions in terms of the wavelength (less than half a wavelength). Thus, for higher frequencies the actual size of the elements is reduced but their individual gain and beamwidth remain constant. Among these elements, dipoles, microstrip patches (circular or square) and crossed slots can be mentioned.

As frequency is increased, the gain of an array with a fixed number of such elements does not change. Instead, the overall size of the array is reduced. The inter-element separation of approximately half a wavelength is maintained in order to suppress the grating lobes. A higher gain is achieved by increasing the number of elements. Such an increase does not add significantly to the cost of a mechanically steered array. The cost increase can be substantial, however, for an electronically steered array where the number of relatively costly phase-shifters increases accordingly.

In either case, the increase in gain is accompanied by an increase in dividing network loss. This beamforming loss is, in general, proportional to the logarithm of the number of elements, while gain increases linearly with the number of elements; therefore, the overall effect is a net increase in gain.

5.2 BASIC PERSONAL TERMINAL ANTENNAS

5.2.1 IMPACT OF 20/30 GHZ FREQUENCY SEPARATION

Since there are no official frequency assignments for the PASS system at present, the question arises as to whether the use of the uplink (transmit) and downlink (receive) frequencies at around 30 and 20 GHz, respectively, may cause a problem in the design of the user antenna. We illustrate the problem with respect to a planar array antenna (with electronic steering in azimuth and elevation, or just mechanical steering in azimuth). No design problem exists if separate antennas are used for the two modes of operation. Employing two antennas, however, in addition to an increase in the total weight and size, could be much more expensive. A single antenna covering both frequencies is preferable. In this case, the transmit and receive antennas will use all or parts of the same aperture.

In general, two different types of user antennas can be considered: reflectors and arrays. The reflector antenna, due to its nonconformality and also due to the fact that it would require strictly mechanical steering, is less desirable from an operational point of view. However, in general, it has some strong points: it is broadband (in terms of frequency), has relatively low feed network loss, and is generally less expensive. Its bandwidth, of course, is determined by the feed. The feed, which can be either a horn or open waveguide, or a small array of elements such as microstrip patches, does not present any major problem in providing the necessary bandwidth.

The planar array of a number of radiating elements may be a more suitable antenna candidate. Although the array can also be steered strictly mechanically in both elevation and azimuth, it is more likely that in order to keep conformal, it will be electronically steered in both azimuth and elevation or at least in elevation with mechanical steering in azimuth. In either case two approaches are possible.

In one approach, broadband array elements can be used to provide operation across the total bandwidth from 20 to 30 GHz. This kind of frequency coverage is not really needed or required, since only a very small frequency band around each of the two frequencies is utilized in the system. Furthermore, such a broad bandwidth is hard to achieve using relatively simple planar elements.

However, this approach is relatively simple to implement, if the receive and transmit operating frequencies are very close to each other with only a few percent total bandwidth (e. g., 20/21.5 or 30/32 GHz). A 40/44 GHz system, with a bandwidth of less than 10 percent, would also fall in this category; namely, the same elements can be used to cover both frequencies.

A better approach is to use collocated elements such as dual stacked microstrip patches or other dual resonant radiating elements which cover very narrow frequency bands (on the order of 1 percent) centered at each of the two operating frequencies. This approach has the added advantage of providing an inherent isolation of up to 20 dB between the transmit and receive frequencies, thereby reducing the isolation requirements of the diplexers.

In another approach, the receive and transmit arrays can be separate but interleaved to occupy the same aperture. This approach has the advantage of relatively simple element design since elements in each array need to operate over a relatively small frequency band. Furthermore, a much better isolation than the collocated elements arrangement can be achieved. However, due to the increased spacing required between the elements of either array in at least one direction, electronic scanning in that direction will create high grating lobes, unless substrates with very high dielectric constant are used to reduce the element size and, hence, spacing. In general, the interleaved arrangement is most suited to a fully mechanically steered array or a hybrid mechanical/electronic scan array with mechanical scanning in the interleave direction.

In either approach, a major problem is the difference in inter-element separation at the two frequencies, in terms of wavelength, which could cause high grating lobes at the higher frequency, particularly for beams steered to low elevation angles. According to the array theory, if the array elements in a regular grid have a large inter-element spacing, grating lobes are produced which manifest themselves as large sidelobes which result in a loss of gain. This problem becomes even more significant for large scan angles. Specifically, the inter-element spacing should be less than or equal to

$$d = 0.5\ \lambda\ /(1 + \sin(\theta)),\ \text{for uniform rectangular grid,} \qquad (8\text{-a})$$

and

$$d = 0.577\ \lambda\ /(1 + \sin(\theta)),\ \text{for uniform triangular grid,} \qquad (8\text{-b})$$

in order to completely prevent the presence of grating lobes. The spacing must be definitely less than twice the above values so that the peak of the first grating lobe does not enter the picture. In Eqs. 8-a and 8-b, θ is the scan angle from zenith (or broadside of the array). For a broadside array (zero scan) the above limits reduce to 0.5 and 0.577 wavelength, respectively, and decrease as the scan angle is increased. Of course, the above values are based on the assumption of isotropic (uniform) element patterns. The natural taper of an actual element would reduce the grating lobe levels.

A representative case is illustrated in Figure 2. A linear array of six elements is considered. Two microstrip patches are stacked at each element position for 20 and 30 GHz performance. This array can be part of a complete planar array. We are, however, concerned with its performance in the plane of beam scanning in elevation.

Figure 3 shows the broadside and scanned patterns of the linear array of six elements with 0.6 cm inter-element spacing. This spacing translates into 0.4 wavelength at the 20 GHz (with 1.5 cm wavelength), and the corresponding spacing for the collocated elements at 30 GHz (with a wavelength of 1 cm) is 0.6 wavelength. This is quite acceptable for the broadside array. However, for the beam scanned to 70 degrees from zenith (to provide coverage at 20 degree elevation) this is far larger than the 0.258 wavelength limit obtained from Eq. 8-a and even larger than the absolute limit of twice that value, i.e., 0.516. In the plots, we have assumed that each element has a half-power beamwidth of 90° at 30 GHz and 135° at 20 GHz.

It may be noted that the higher taper of the narrower element beamwidth at higher frequency partially compensates for the higher array grating lobe at this frequency. As can be seen, the performance at 20 GHz is satisfactory for both the scanned and non-scanned cases. For the 30 GHz case, however, the grating lobe is even higher than the main lobe and not acceptable.

A better result is obtained if the inter-element spacing is reduced to 0.5 cm. In this case, the spacing is 0.33 λ at 20 GHz and 0.5 λ at 30 GHz. This provides a more acceptable performance as shown in Figure 4, although the backlobe for the 30 GHz scanned case is still relatively large. It can be further reduced by amplitude tapering of the array elements. Also, as the number of elements is increased, the grating lobe effect is further reduced as long as the spacing is less than twice the value given in Eqs. 8-a and 8-b.

Furthermore, by introducing non-uniformity in the array lattice and breaking the symmetry of the configuration, one can reduce or neutralize the grating lobes at the expense of complications in the mechanical design and fabrication.

It should be noted that a reduction of inter-element spacing to accommodate the higher frequency, causes the spacing at the lower frequency to be much less than half a wavelength, and since the element size is typically somewhat less than half a wavelength this may seem to create a problem. This problem, however, can be solved by dielectric loading of the element. Thus, by increasing the dielectric constant the element aperture can be reduced to fit the available spacing.

In any case, as long as the total array aperture is used for operation at both transmit and receive frequencies, the resultant array pattern will be narrower and have a higher gain at the higher frequency (30 GHz). If required, it is possible to employ only an inner subset of the array elements at the higher frequency, in order to achieve the same beamwidth and gain as the lower frequency.

In conclusion, it is feasible to obtain reasonable antenna array performance at 20/30 GHz by the use of, for example, dual-stacked microstrip patch elements providing coverage at both frequencies. A simpler design can be employed, however, if the frequency separation is less than 10 percent, for example at the 40/44 GHz range. The latter system will also result in much smaller antenna dimensions for the same gain requirement.

5.2.2 PARAMETRIC STUDIES: GAIN, SIZE, WEIGHT

As an aid in deciding the size, weight and gain of the user antenna, trade-off studies have been performed and will be graphically presented. The emphasis here is on a planar array with a number of identical elements on a uniform grid.

Assuming an inter-element separation of approximately 0.5 and 0.577 wavelength, for the square and hexagonal (equilateral triangular) grid arrays, respectively, the total number of required elements as a function of the array diameter is given by

$$N \approx \pi\,(D/\lambda)^2, \quad \text{for a circular array, square lattice,} \tag{9-a}$$

$$N \approx 4\,(D/\lambda)^2, \quad \text{for a square array, square lattice,} \tag{9-b}$$

and

$$N \approx 0.25 + (1.5\ D/\lambda)^2, \text{ for a hexagonal lattice} \tag{9-c}$$

The case of a circular array with a square grid is graphically shown in Figure 5.

The gain of the planar array with a beam scanned θ degrees from the zenith is approximately given as

$$G = \eta\ (4\ \pi\ A\ /\lambda^2)\ \cos(\theta) \tag{10}$$

Usually it is assumed that a planar array is more efficient than a reflector antenna system because there is no illumination and edge taper loss is involved. For a well optimized reflector design these two losses cause an efficiency factor of about 0.8 (1 dB). As we shall see, as the number of elements in an array increases, the feed distribution network loss can be substantially higher. The array efficiency, η, is composed of three parts:

$$\eta = \eta_{el}\ \eta_{taper}\ \eta_{bfn}, \tag{11}$$

in which η_{el} is the array element loss which is relatively low and in the range

$$\eta_{el} \approx 0.9 - 0.99 \text{ dB}, \tag{12-a}$$

and η_{taper} is array taper which may be introduced in order to reduce the sidelobe levels and may be in the range

$$\eta_{taper} \approx 0.8 - 1 \text{ dB}, \tag{12-b}$$

and finally η_{bfn} is the beam-forming network loss. This loss in general can be given as

$$\eta_{bfn} \approx 3.32 \log (N)\ L_{div} + L_{\phi}, \tag{12-c}$$

in which N is the number of array elements, L_{div} is the equivalent loss per two-way divider, and L_{ϕ} is the loss in the phase shifter. For an n-bit phase shifter the loss is n times the loss per single bit phase shifter. The divider loss is calculated based on the assumption of a binary tree divider network. At Ka band frequencies, loss per two-way divider can be in the following range:

$$L_{div} \approx 0.3 - 1 \text{ dB}.$$

Figure 6 shows the dividing network loss as a function of the number of array elements N based on the assumption of an optimistic figure of 0.3 dB per divider. It is seen that the loss in dB increases as a logarithmic function of the number of elements, and for a few hundred elements could reach a few dBs, much more than the illumination and spill-over loss in a reflector antenna.

The phase shifter loss at the Ka band frequencies can be even more significant. Digital phase shifters presently under development can have several dBs of loss per bit. Instead, one can use continuously variable ferrite phase shifters with relatively little loss (a few tenths of dB). Unfortunately, this type of phase shifter is bulky and does not easily lend itself to integrated circuit manufacturing techniques.

The beamforming network loss can be altogether avoided if one implements an active array antenna. In an active array, a TR (Transmit/Receive) module will be located behind each radiating element or a small subarray of such elements.

In this way, the loss in the beamforming network will not be a high power loss in the transmit mode, and also will not contribute significantly to the receiver noise temperature (see Section 5.2.3). Such an active array can be manufactured using MMIC (Microwave Monolithic Integrated Circuit) techniques. The cost and complexity associated with such a design is presently quite significant, but may be substantially reduced in the next few years.

Figure 7 shows the gain of a completely mechanically steered array. No phase shifter loss and no beam scan loss are present, since it is assumed that the array is mechanically steered in both azimuth and elevation. Figure 8 shows the gain of both the passive and active (without the network and phase shifter loss) phased arrays versus the number of elements. The curves are based on Equations 10, 11, and 12. Three bit phase shifters with a loss of 2 dB per single bit is assumed.

The issue of the weight of the array antenna is more complicated and requires more detailed designs before accurate numbers can be produced. However, based on prior experience and some rough estimates regarding the components, the weight is estimated in the range of 5 to 10 g/sq cm (0.07 to 0.14 lb/sq in.), with the lower figure closer to a phased array design while the higher is closer to a mechanically steered design.

5.2.3 GAIN AND FIGURE OF MERIT (G/T)

G/T is a figure of merit to measure the performance of a receiving system. For active array antennas, the array configuration (i.e., the order of the amplifiers and the dividing/combining layers) impacts the overall system G/T. A study has been performed and is documented in Appendix I.

5.2.4 DESIGN DATA FOR SELECTED ANTENNA CONCEPTS

In general, from beam pointing considerations, we identify five feasible types of design for PASS user antennas in order to provide the required CONUS coverage, i.e., 360 degrees in azimuth and 20 to 60 degrees in elevation:

i) Fully electronically steered planar array.

ii) Fully mechanically steered in both azimuth and elevation. The antenna in this case can be either a planar array or a reflector antenna.

iii) Hybrid mechanically/electronically steered planar array. In this case, the beam can be rotated mechanically in azimuth, while beam tilt in elevation can be provided by electronic scanning or switching.

iv) Mechanical steering in azimuth with a fixed broad beam in elevation.

v) Electronic scanning or switching in elevation with a full 360 degree coverage beam in azimuth direction.

In this section, we present some design data for a fully electronically steered antenna and a fully mechanically steered antenna. Only gain and pattern information will be provided.

For planar phased array design we consider a uniform equilateral triangular (i.e., hexagonal) grid which has the highest array packing efficiency, namely, it requires the smallest number of elements per given area (see Eqs. 9(a-c)). Two examples of hexagonal arrays are given in Figures 9(a-b). The total number of elements in such an array is given by

$$N = 3\,m^2 - 3\,m + 1,$$

in which m is the generating number of the hexagonal grid and is equal to the number of elements on each side of the hexagon. Figure 10 provides far-field patterns for the 91 - element array of Figure 9(a).

A rectangular array can be used in a fully mechanically steered array. Both azimuth and elevation steering are provided. Figure 11 shows a possible layout of the array configuration while Figure 12 shows its mechanical design layout and Figure 13 provides typical far-field patterns.

A reflector antenna can also be used for the mechanically steered case. However, reflectors are usually used for gain of 30 dB or higher. Typically, the dimensions of the

reflector must be larger than about 10 wavelengths. Otherwise, the performance of the antenna suffers both in terms of the increased sidelobes as well as lower gain.

5.2.5 CRITICAL TECHNOLOGIES AND DEVELOPMENT GOALS

The aim of user antenna development is the design and mass production of very small, light weight, and economical units with good performance across the frequency band of operation and over the entire geographical region of interest, namely CONUS. As has been revealed in the process of this study as well as in the experience gained in the MSAT-X project, there are a number of challenges that have to be overcome.

One group of challenges has to do with the optimization of the antenna pattern characteristics, such as gain, polarization performance, and sidelobes and backlobes, given the constraints of small size and portability. Another group of challenges is associated with the requirement, selection and specification of RF components and materials that are or will be of a mature technology in the near future at relatively low prices.

Amenability of the design to integration and ease of fabrication in a mass production environment also falls within this category. The procurement of small, reliable and low-cost mechanical moving parts such as motors, rate-sensors, etc., and the development of efficient techniques for acquisition and pointing in one or two dimensions constitute a third category of challenges.

We identify the following technologies as some of the more important ones in reaching the objectives of this program.

1) **Necessary software development:** There is already a vast base of antenna analysis, synthesis, and design software presently available at JPL. However, these tools need to be further refined, modified and optimized for the kind of antenna performance goals that are relevant to the PASS system.

   One objective is to provide a complete characterization of ground plane effects in the antenna pattern analysis. Also needed will be the development of fast and efficient pointing software for the acquisition and tracking of the satellite. This is particularly significant considering the ambulatory environment of the PASS user antenna, requiring fast and reliable tracking in azimuth and elevation.

2) **New element and array concepts:** Both mechanically as well as electronically steered planar array antennas are prime candidates for the user antenna. As has been discussed, a very large number of radiating elements may be required to achieve the relatively high gains required at 15 to 20 degrees elevation. New and innovative element designs with very broad beams or tilted beams with relatively high gains at low elevations can reduce the number of needed elements. New sub-array and

arraying concepts to reduce the number of required elements and reduce the side and back lobes are also needed.

3) **Low loss, reliable and inexpensive RF components:** In both electronically and mechanically steered array design at Ka band frequencies, design and development of low-loss power divider/combiners is important, since the overall loss depends on the number of elements and the loss per divider unit. Reducing the two-way divider/combiner loss to 0.1-0.3 dB levels will significantly enhance the PASS user antenna development.

Of more concern are the phase shifters needed in the electronically steered phased arrays. There are continuously variable ferrite phase shifters of relatively low loss (a few tenths of dB) with potential application to Ka band frequencies. These are, however, relatively bulky and do not easily lend themselves to MMIC design and fabrication techniques. Solid state digital phase shifters presently available or under development, on the other hand, show unacceptably high losses (a few dB per bit), although they are suitable for Monolithic Integrated designs.

Advances in either category are required in order to make a phased array approach economically and technically feasible. Solid state switching elements required for electronically switched beams are also in the category of components which need to be made at low cost with high reliability and low loss.

4) **Low cost and reliable T/R modules:** High circuit losses introduced by the dividers and phase shifters in the array beam forming networks can be overcome by the introduction of T/R (Transmit/Receive) modules at the element or sub-array level. Development of low cost and reliable T/R modules within the MMIC configuration is an essential part of making phased array antennas attractive for PASS and similar applications.

5) **Small, inexpensive, and reliable pointing hardware:** Due to the mobile or ambulatory nature of the user antenna, design and selection of appropriate satellite acquisition and tracking hardware (or pointing system hardware in general) are as important as the RF subsystem design.

For instance, the development of small or miniature motors, preferably with a flat or pancake design no more than a few inches in diameter, with sufficient torque (more than 15 to 20 oz.-in.), reliable long term performance and available at low cost (less than $100 in large quantities), is a major component of a successful design. So are the rotary joint, the support bearings, and particularly inexpensive rate sensors with accurate and reliable performance. Again, the emphasis here is on the miniaturization as well as low cost.

5.2.6 RECOMMENDATIONS

Based on a literature survey and study performed in the course of this work we make the following recommendations for the development of basic personal terminal antennas:

i) The most likely candidate for a personal terminal in the next five years is a mechanically steered antenna (with tilted aperture). The fully mechanically steered array with automatic azimuth rotation and elevation tilt capability is perhaps the most promising in terms of cost, complexity and reliability. Both planar passive arrays as well as reflector-type antennas can be employed in such a system. Transmit gains of 20 to 25 dB can be expected from these antennas, with a receive G/T of 8 to 10 dB an achievable goal.

ii) As the MMIC technology matures and low loss, relatively low cost phase shifters and solid state amplifiers with acceptable efficiency, power handling capability, and relatively low cost with high packaging efficiency become available, a tilted or planar array with mechanical rotation capability for azimuth acquisition and tracking, and electronic scanning in elevation, becomes a feasible option. In such a system only linear sub-arrays of the total array may require phasing and T/R module, and hence the complexity and required packaging efficiency is well below a full fledged phase array design.

iii) Finally, in about 5 to 10 years the maturity of MMIC technology may be such that the idea of a fully electronically steered planar array antenna with T/R modules at each radiating element, providing a very low loss and hence low noise and high gain antenna in a small package of the order of 10 cm in size with gains of the order of 25 dB or higher and a G/T of better than -5 dB, will achieve economic feasibility. This, however, presupposes an intensive effort on the part of NASA and private industry to actively pursue and continue research and prototyping in the K_a band and higher frequency regimes.

5.3 USER ANTENNA RADIATION SAFETY CONCERNS

An important consideration in the design of the user antenna for the Personal Access Satellite System is the safety hazards associated with the radiation at Ka band frequencies. This is because of the proximity of the antenna to the user (from a few inches to a few feet), relatively high gain of the antenna, and lack of sufficient information on the effects of radiation at 20/30 GHz frequencies. There exists an ANSI document outlining safety standards for human exposure to RF radiation [2] and many papers and documents studying various aspects of the subject (see, e.g., [3]). Appendix II presents a short study of this subject with useful information on the RF radiation hazards in general and with specific application to the PASS system. It also indicates the need for further investigation, perhaps by an outside agency (e.g., a university), for reaching a satisfactory conclusion.

Here we present a short summary of the main issues of concern and some plots that can be useful in relating the antenna input power and the radiation levels (RF field intensity) for various antenna gains and distance from the antenna to the user.

i) In many antenna applications the transmitting antenna is far from the system users. Therefore, the radiation effect on the user is either nonexistent or minimal. In any case the user is in the far field of the antenna. The plot in Figure 14 gives a definition of different regions of an antenna in terms of the antenna size, wavelength and distance from the antenna aperture. As can be seen in this figure, for antenna apertures of about 5 to 10 centimeters (5 to 10 wavelengths at the 30 GHz transmit frequency), a user at a distance of a few inches from the antenna would be in the mid to near field of the antenna.

Characterization of the field in the near-field region is usually more complicated than the far-field region. However, the main point of interest here is the fact that in this region the field has a substantial longitudinal component (in the propagation direction) in addition to the transverse components which are also present in the far field. Studies have shown [4] that, in general, the longitudinal field component does not have any noticeable adverse effect on biological tissue and only the transverse field components need to be considered. From this it can perhaps be concluded that for a far field and a near field of comparable strength, the former has more deleterious effects. This is an area that needs further study.

Furthermore, due to the proximity of antenna to the user, the user body becomes a scatterer of energy and distorts and redistributes the overall field pattern. This problem has not been dealt with in any substantial degree. A simple approximation is to assume the same field distribution with and without the presence of the nearby objects.

ii) The RF radiation effects can be divided into two general categories: the heat effects and the chemical/cellular effects. Most studies have shown that only heat effects (a rise in temperature in the body tissues) have significant adverse effects on the biological tissues. Most of the chemical effects are either insignificant and/or reversible.

iii) Two criteria have been developed for characterizing the radiation effects:

The first criterion is related to the exposure of the human body to a uniform field, namely whole body exposure. This is an average, and according to established standards, the maximum power density per unit of area of the human body should not exceed a specific level (e.g., 5 mW/cm^2 at 30 GHz). This is based on the assumption that the average Specific Absorption Rate (SAR), namely the time rate at which electromagnetic energy is coupled to the body, will not exceed 0.4 W/Kg averaged over the whole body and over a 6 minute period. Figures 15 and 16 provide generic curves for the power density of aperture antennas at various distances from the antenna and for different antenna aperture sizes.

The second criterion relates to the localized effects of the RF field. According to this criterion the spatial peak SAR should be below 8 W/Kg per any one gram of body tissue.

This is a more important consideration when the radiation source is close to the subject of exposure.

iv) Most of the theoretical as well as experimental investigations of the radiation effects, to date, have been performed at frequencies below X-band (8 GHz or less). Only recently there has been an interest specifically in the Ka band region of RF spectrum, although sufficient and conclusive results are not yet available.

Recent findings [5], however, tend to indicate that the problem may not be as critical as some may have suspected and that the radiating safety levels specific to the Ka-band frequency range do indeed fall within the already established standards.

At any rate, should the radiation levels at 30 GHz prove to be excessive, there are certain ameliorative measures that can be taken. Aside from the obvious solution of reducing the transmitted power level which, depending on the system link budget requirements may or may not be feasible, the following measures may prove appropriate:

a) The use of a radome to cover the regions of high intensity radiation near the antenna. As discussed in Appendix II and also observed in Figures 13-14, radiation intensity peaks at a certain distance from the antenna aperture and is a function of the antenna aperture size. The peak of the radiation occurs at a distance of approximately

$$d \approx (1/4)\,(D^2/\lambda)$$

from the antenna aperture. This distance for an antenna with 20-25 dB gain at 30 GHz is in the 5-15 cm range. It may be feasible to enclose this high intensity region within a protective radome.

b) The use of a sensor to detect the presence of objects in the proximity of the radiating antenna and issuing a warning signal and/or possibly turning off the antenna.

In conclusion, due to the proximity of the radiation source (the antenna) to the human head in typical PASS applications, the exposure is at the near field of the antenna and is of a localized nature. Of critical importance is the localized 30 GHz radiation effects on the eyes and the ears. This is a problem that may require additional study. In any case, there are certain measures that may be taken to reduce the effects in the user antenna environment.

REFERENCES

[1] Miles Sue, Editor, Personal Access Satellite System Concept Study, JPL Publication JPL D-5990, February 1989.

[2] American National Standard Safety Levels with Respect to Human Exposure to Radio Frequency Electromagnetic Fields, 300 KHz to 100 GHz, Report No: ANSI C95.1-1982, Prepared by IEEE and US Department of the Navy.

[3] C. H. Durney, et al., Radiofrequency Radiation Dosimetry Handbook, Fourth Edition, Report No: USAFSAM-TR-85-73, Prepared for USAF School of Aerospace Medicine, October 1986.

[4] A. Lakhtakia, M. Iskandar, "Scattering and Absorption Characteristics of Lossy Dielectric Objects Exposed to the Near Fields of Aperture Sources."

[5] USAF Report on Radiation Experiments at 30 and 90 GHz Using Cat's Eyes, to be released in March 1990 by USAF School of Aerospace Medicine.

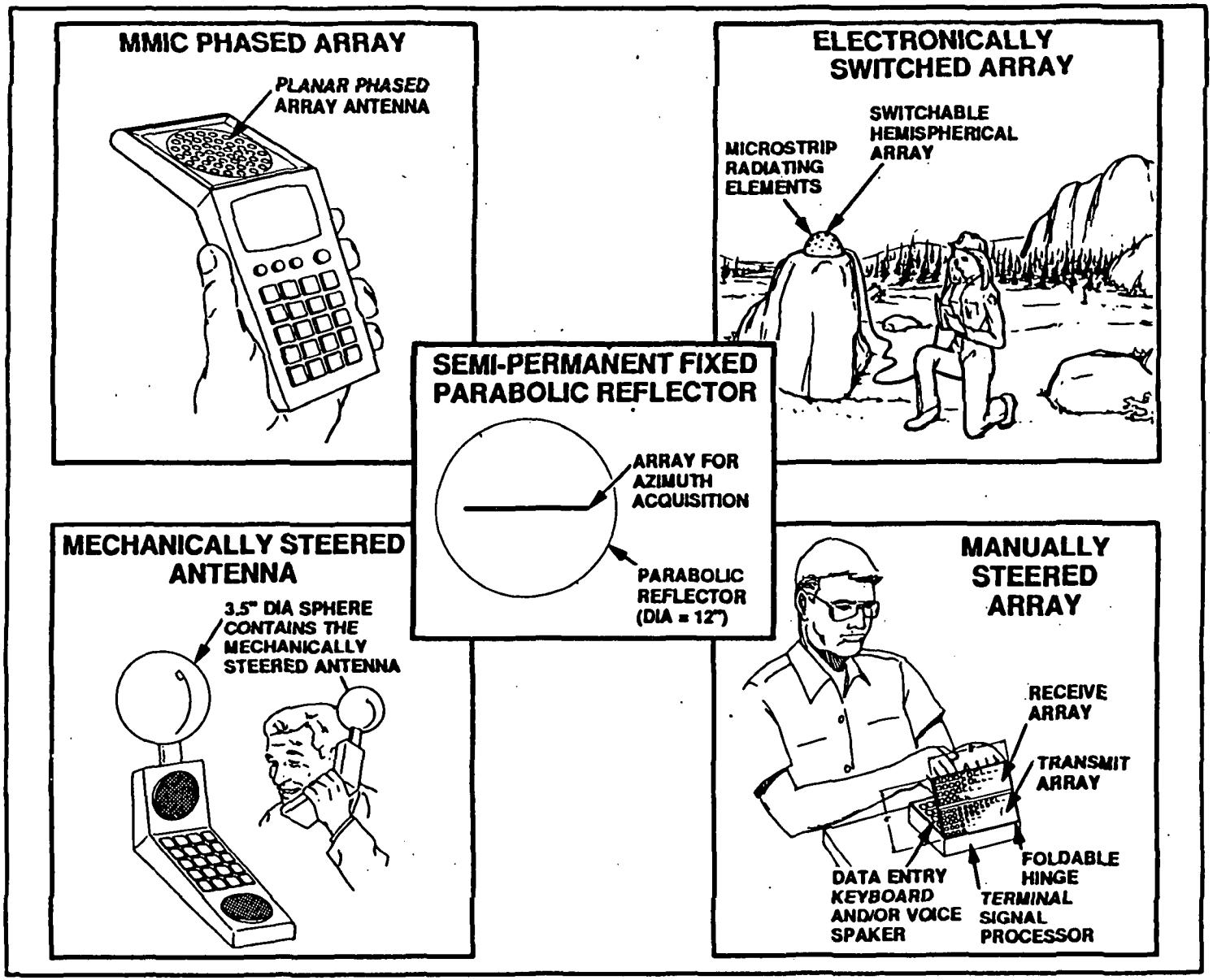

Figure 1. Typical user terminal antenna design concepts (from [1]).

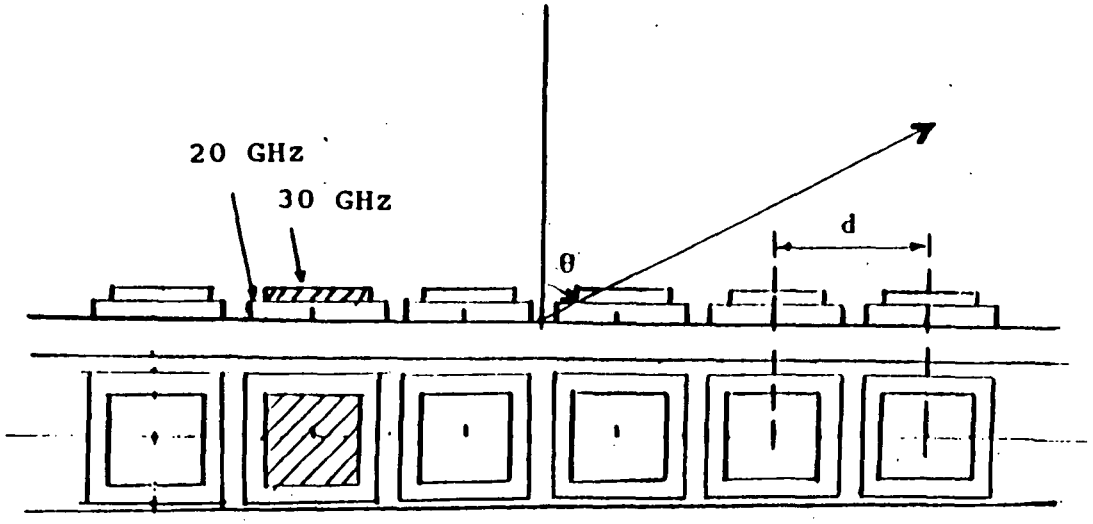

Figure 2. Sketch of a 6-element linear array with collocated elements for 20 and 30 GHz, and inter-element spacing, d.

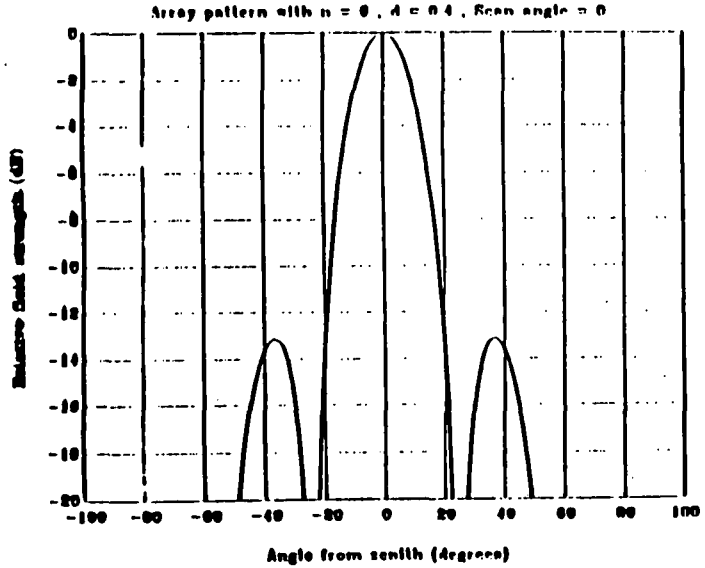

(a) Broadside pattern at 20 GHz

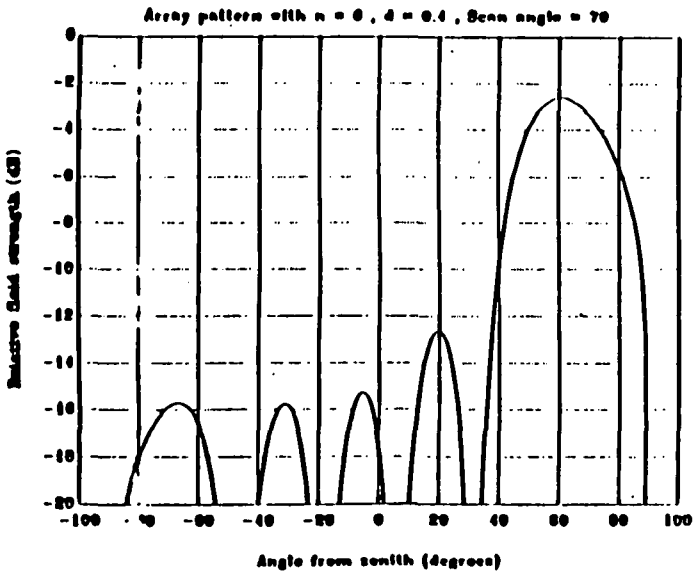

(b) 70° scanned pattern at 20 GHz

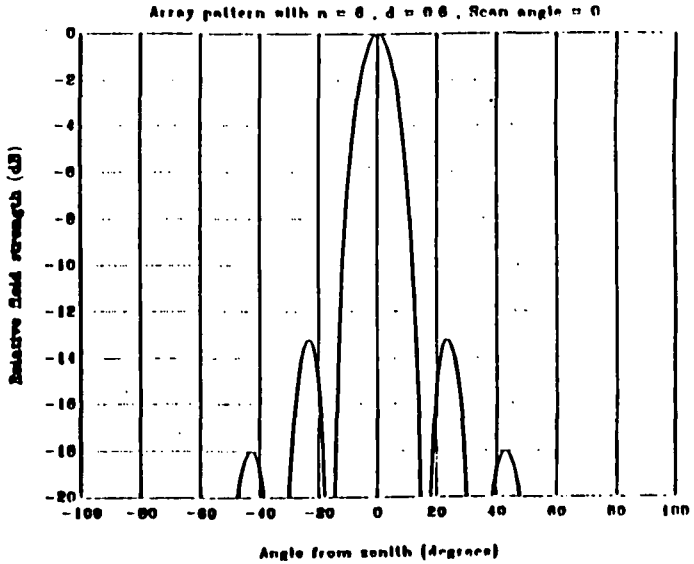

(c) Broadside pattern at 30 GHz

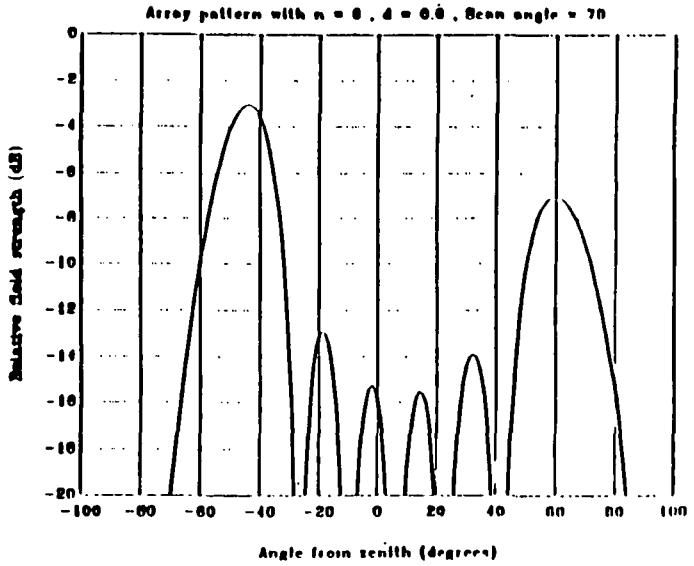

(d) 70° scanned pattern at 30 GHz

Figure 3. Patterns of a six element array at 20 and 30 GHz : 0.6 cm inter-element separation.

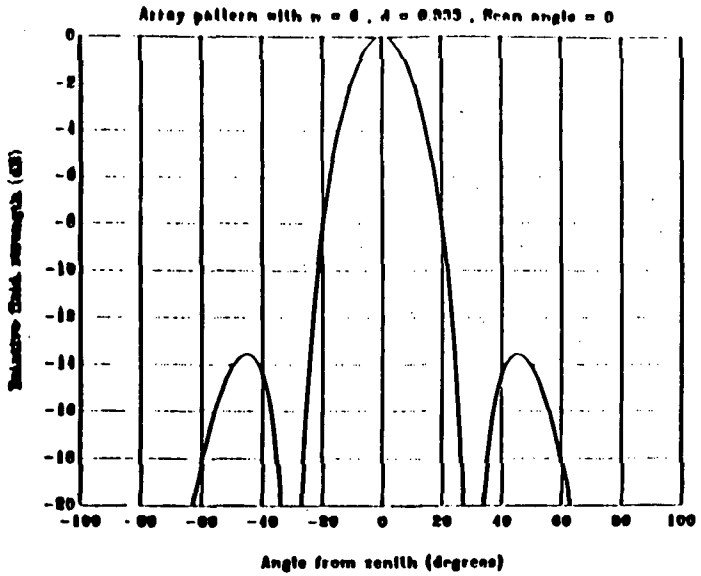

(a) Broadside pattern at 20 GHz

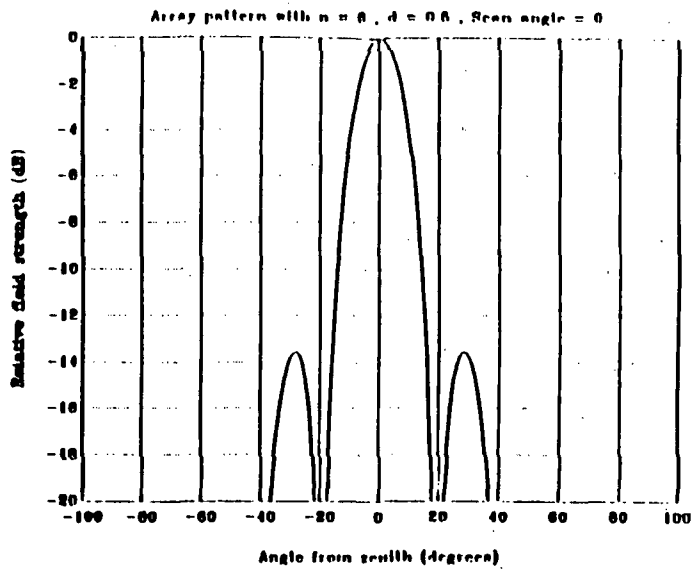

(c) Broadside pattern at 30 GHz

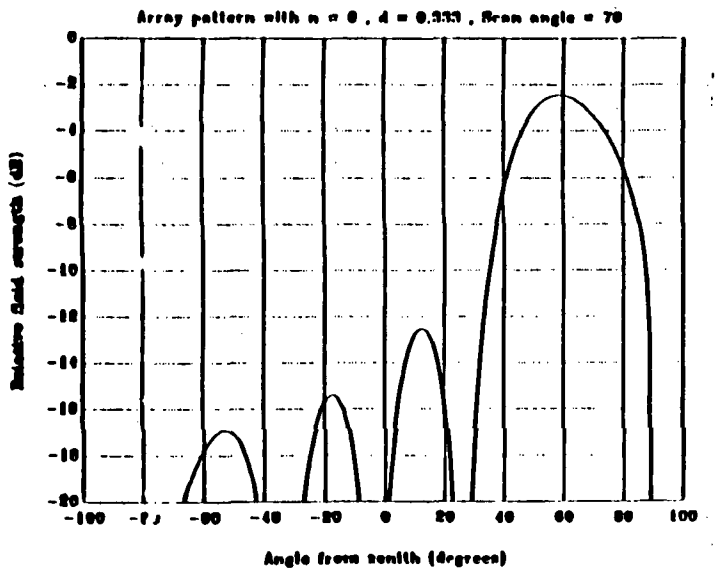

(b) 70° scanned pattern at 20 GHz

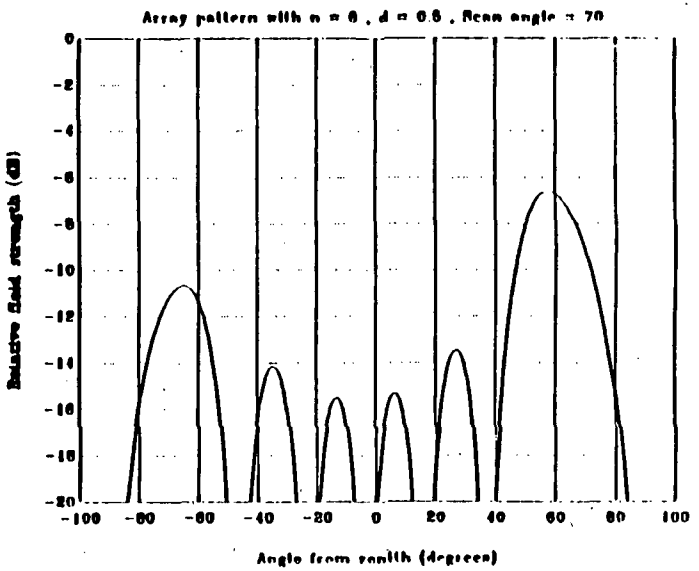

(d) 70° scanned pattern at 30 GHz

Figure 4. Patterns of a six element array at 20 and 30 GHz: 0.5 cm inter-element separation.

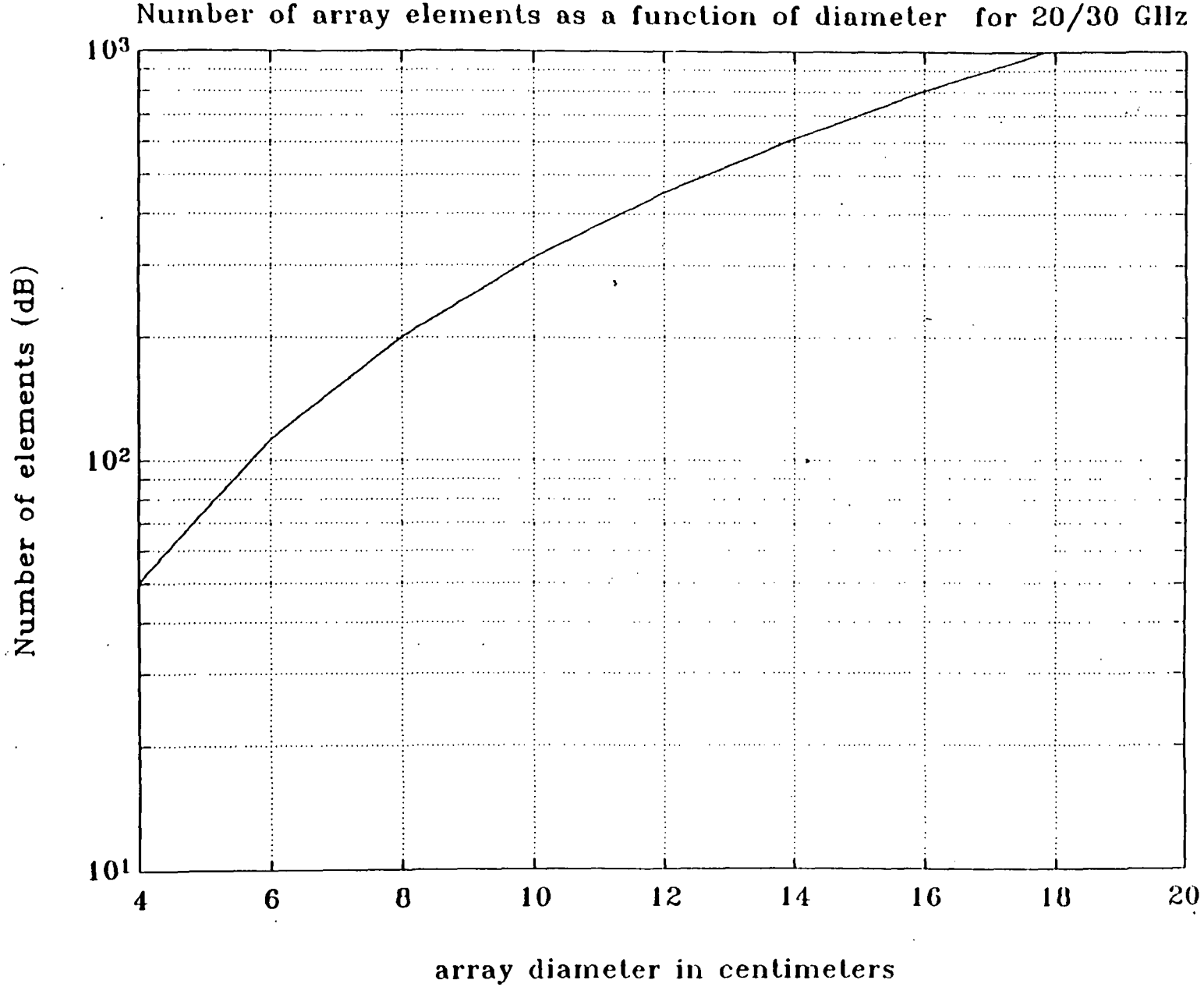

Figure 5. Number of elements versus array diameter in a 20/30 GHz array antenna.

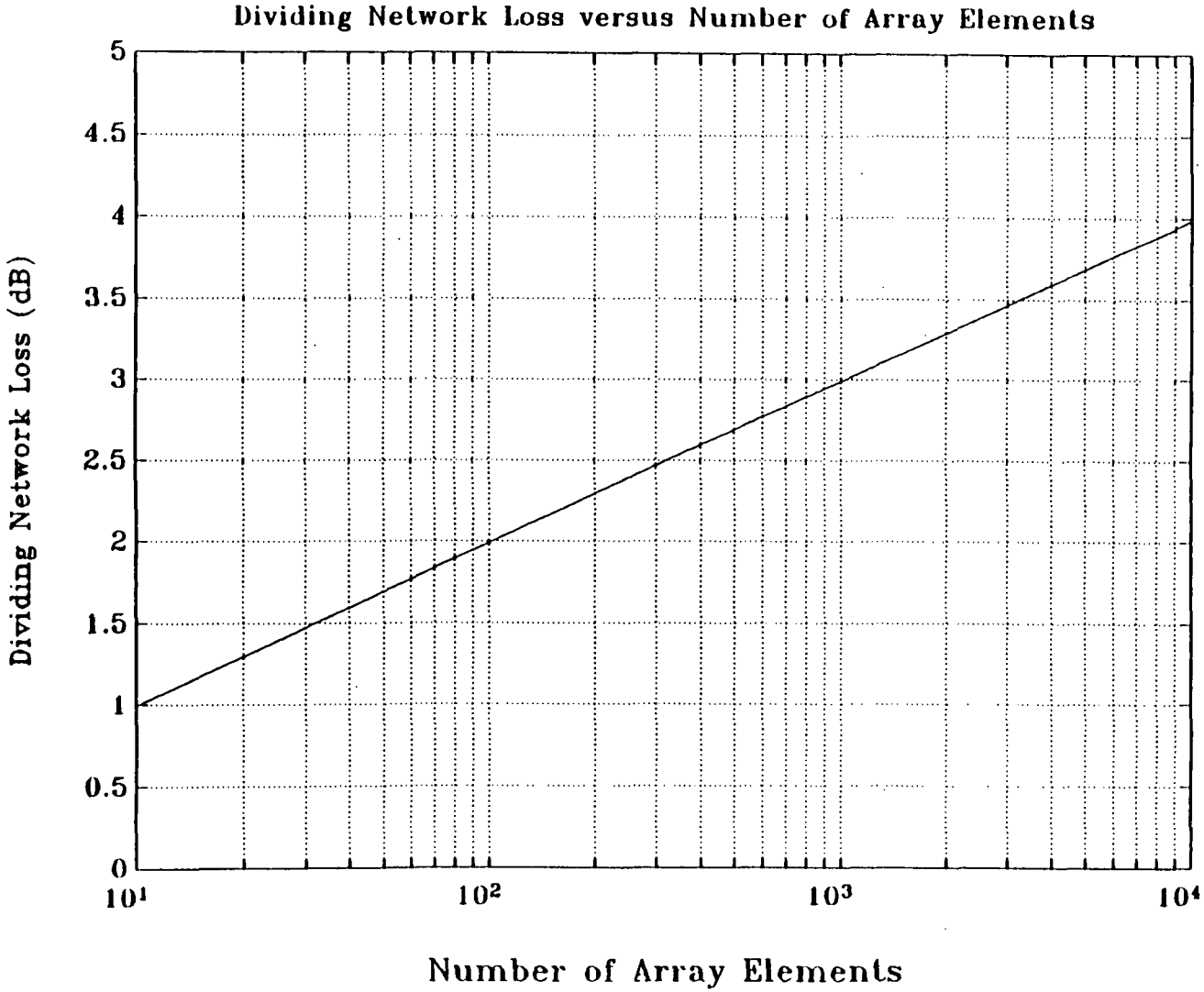

Figure 6. Dividing network loss as function of the number of array elements. 0.3 dB per two-way divider is assumed.

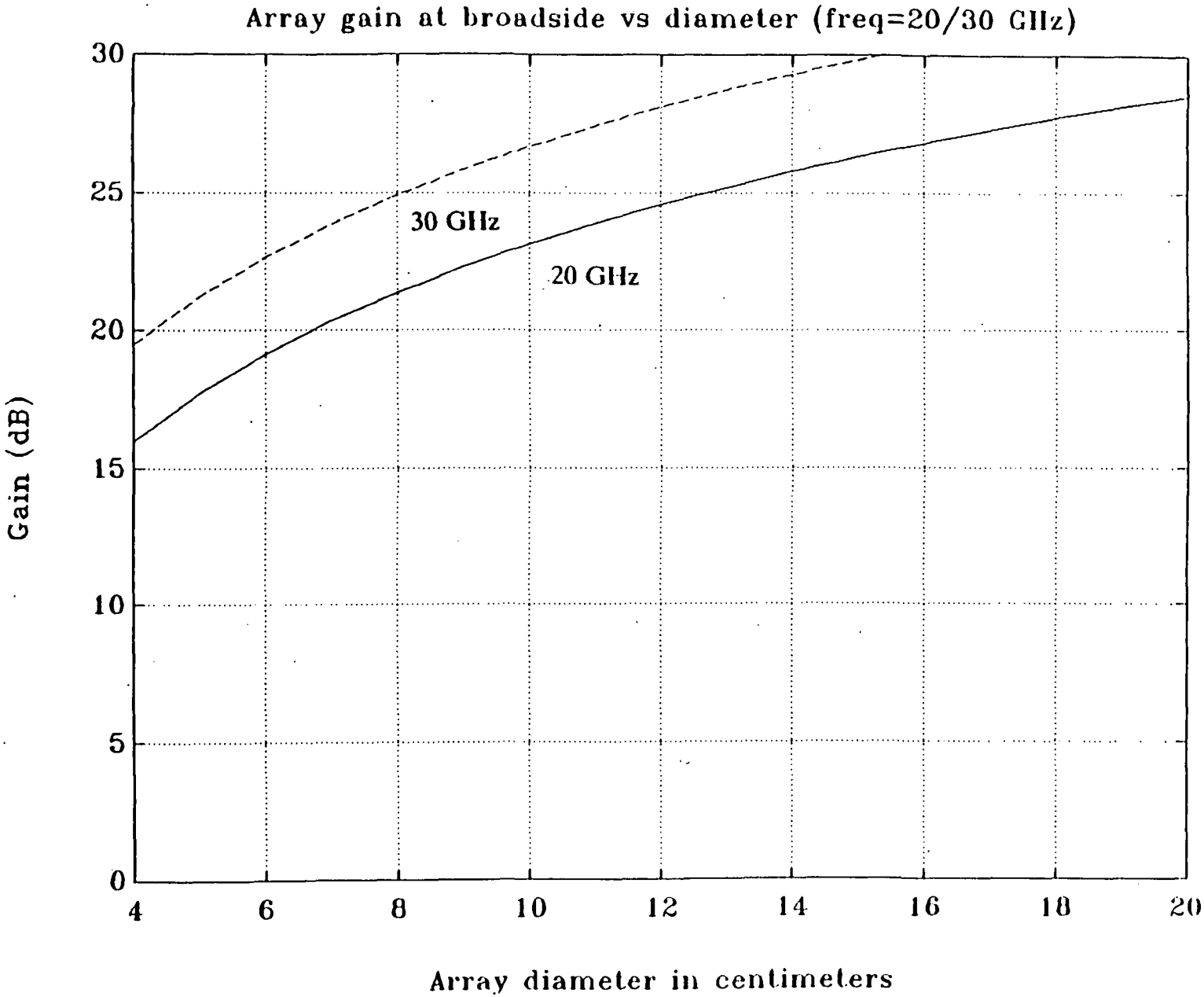

Figure 7. Mechanically steered (in both azimuth and elevation) array gain at 20 and 30 GHz as a function of diameter.

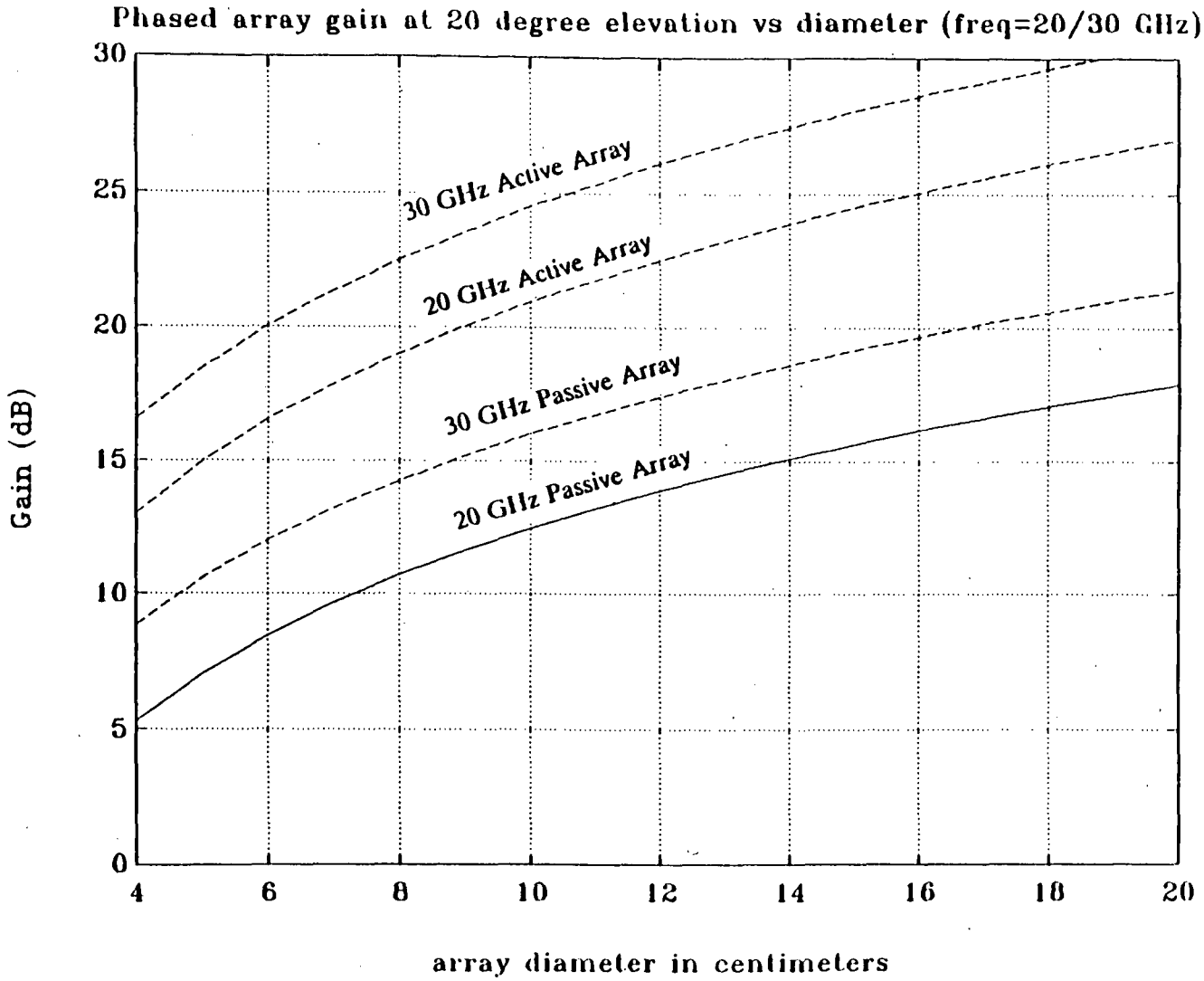

Figure 8. Phased array gain at 20 and 30 GHz as a function of diameter. Both active and passive arrays are considered.

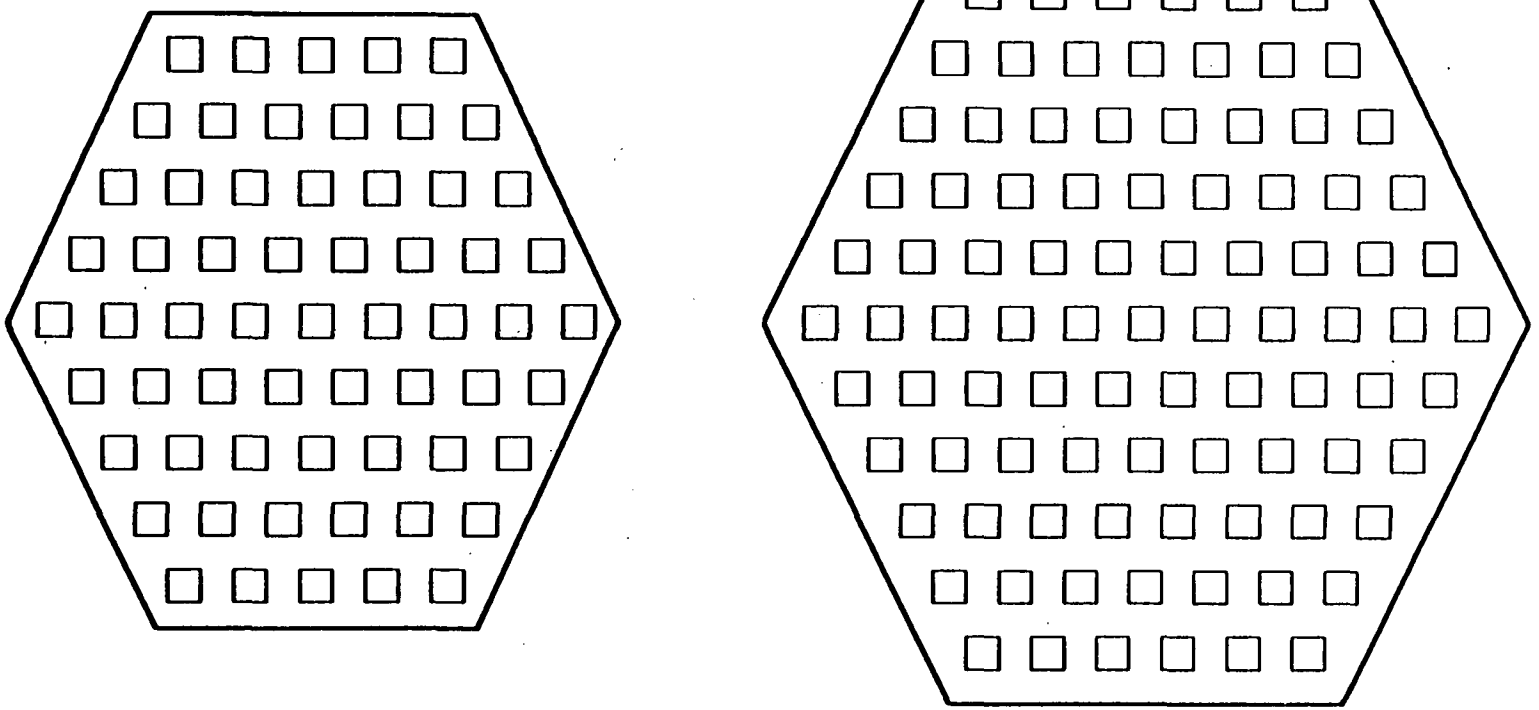

(b) 61 ELEMENTS

(b) 91 ELEMENTS

Figure 9. Hexagonal grid array configuration

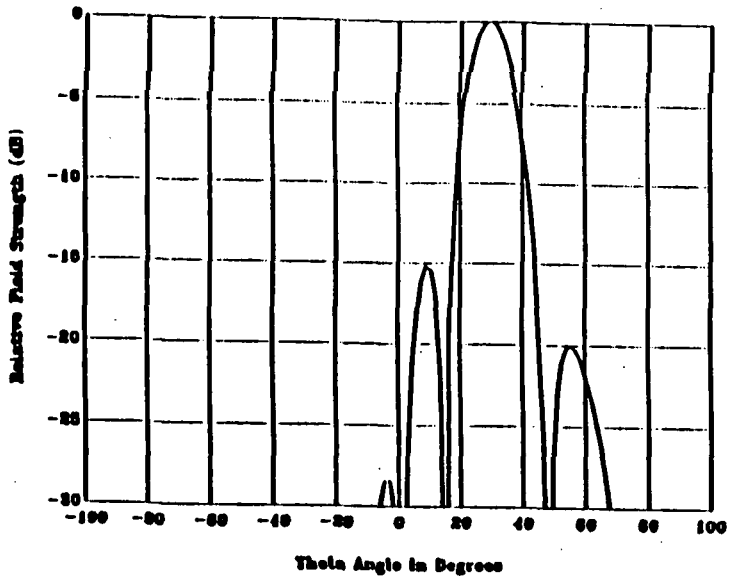

(a) 30 GHz peak gain at 60° elevation = 23 dB

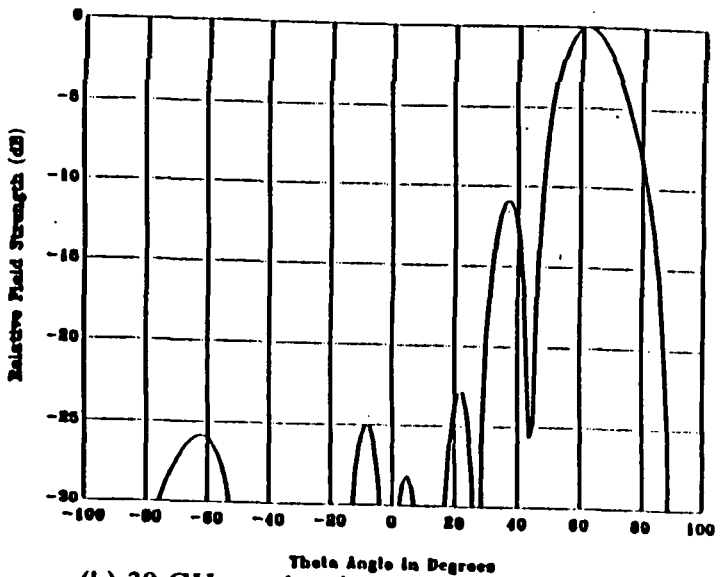

(b) 30 GHz peak gain at 20° elevation = 19 dB

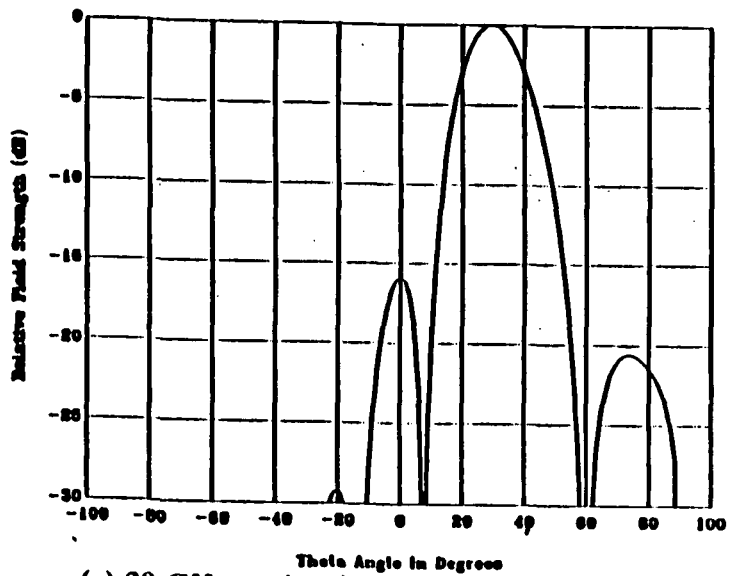

(c) 20 GHz peak gain at 60° elevation = 20 dB

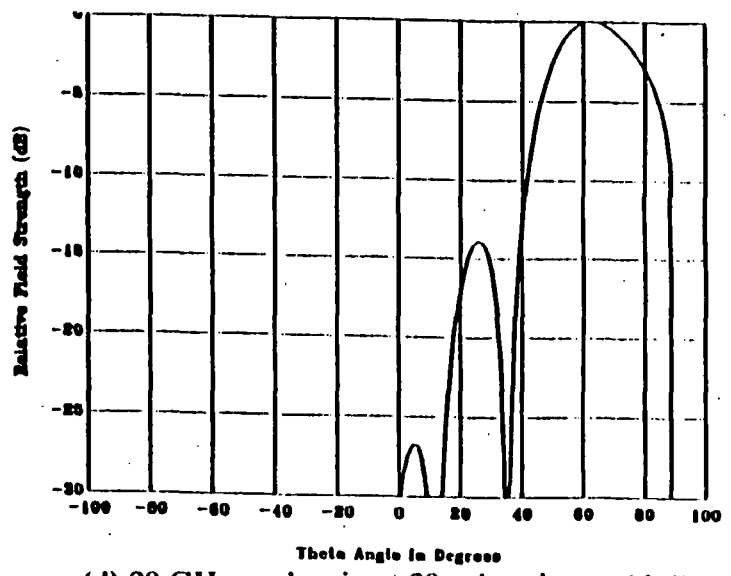

(d) 20 GHz peak gain at 20° elevation = 16 dB

Figure 10. Typical far-field patterns of the 91-element hexagonal grid array for an electronically steered antenna

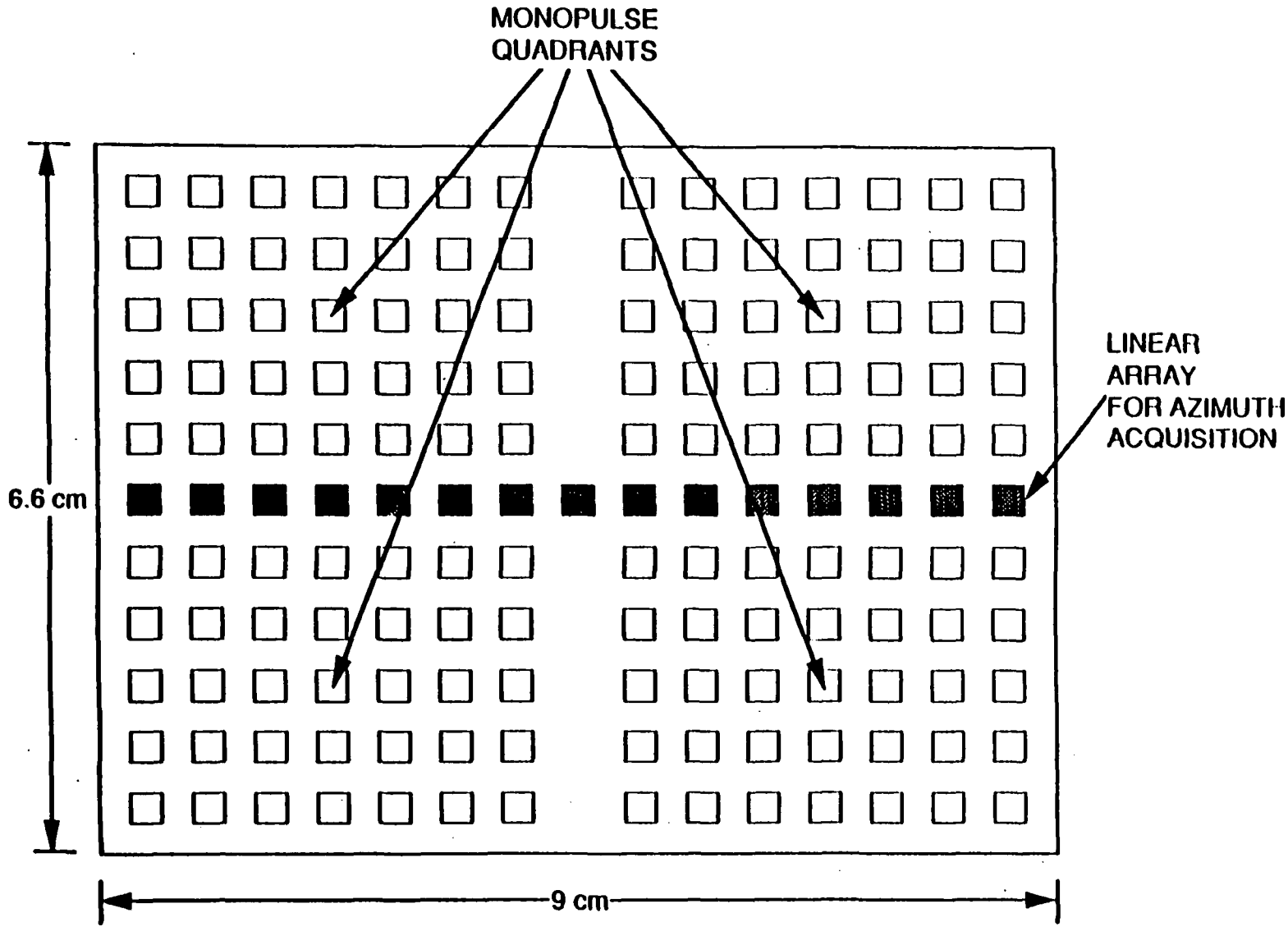

Figure 11. A typical rectangular grid array for a mechanically steered antenna.

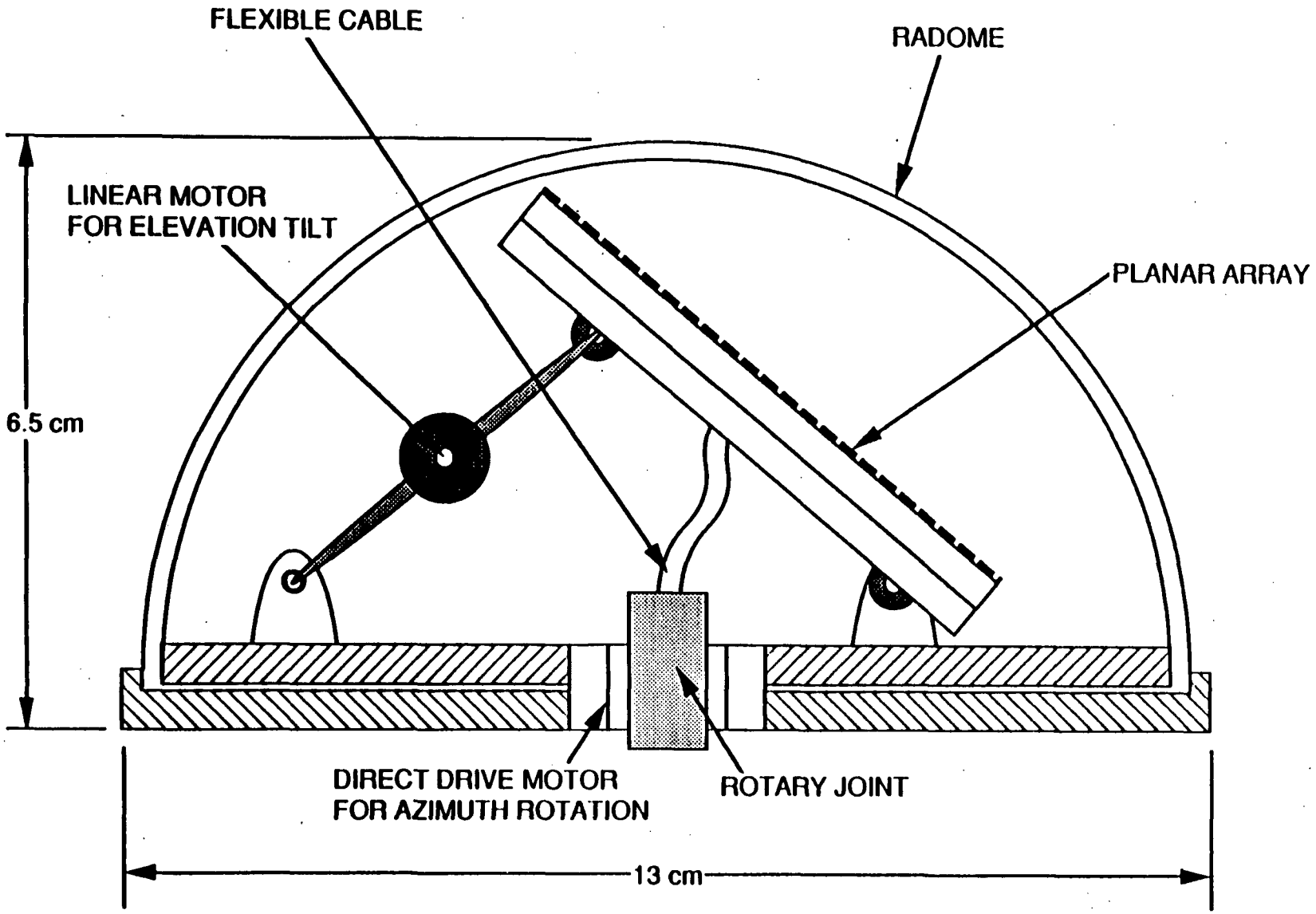

Figure 12. An implementation concept for a mechanically steered antenna.

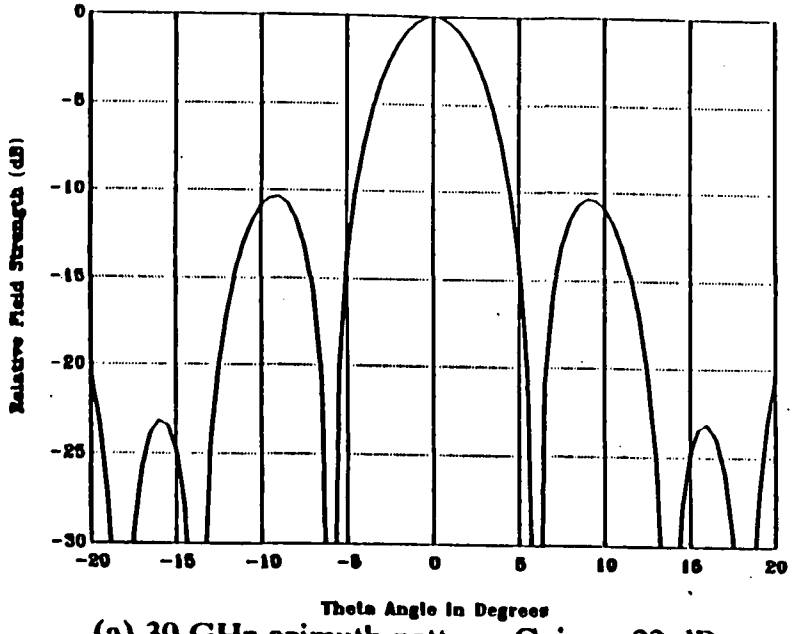

(a) 30 GHz azimuth pattern, Gain = 22 dB

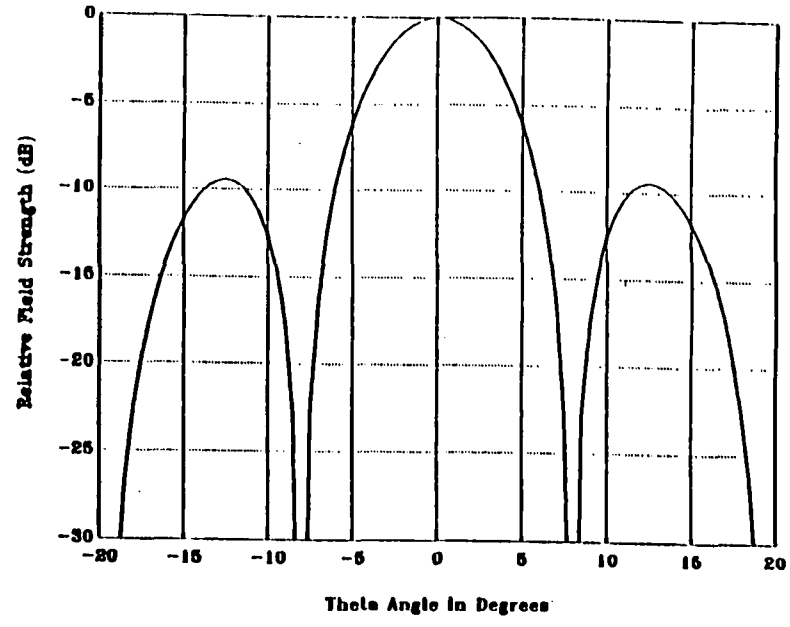

(b) 30 GHz elevation pattern, Gain = 22 dB

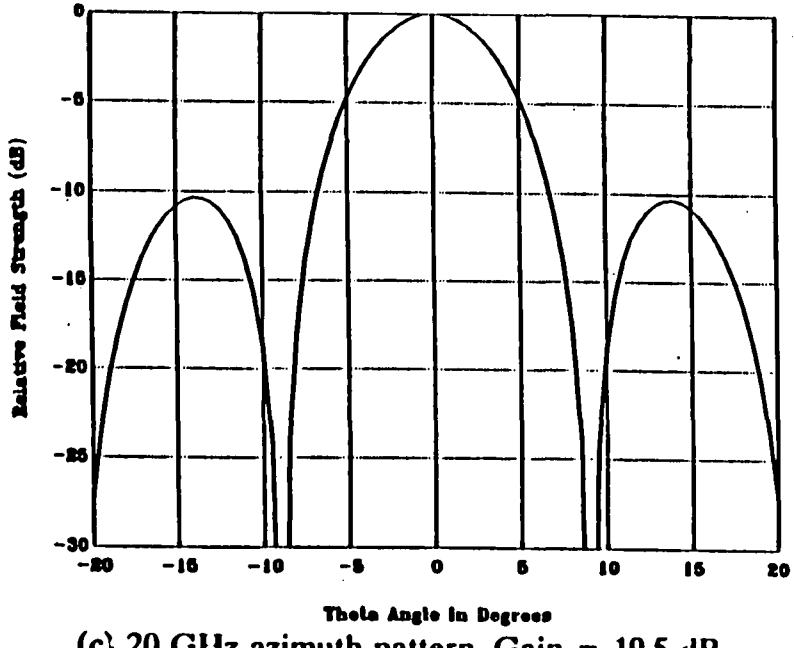

(c) 20 GHz azimuth pattern, Gain = 19.5 dB

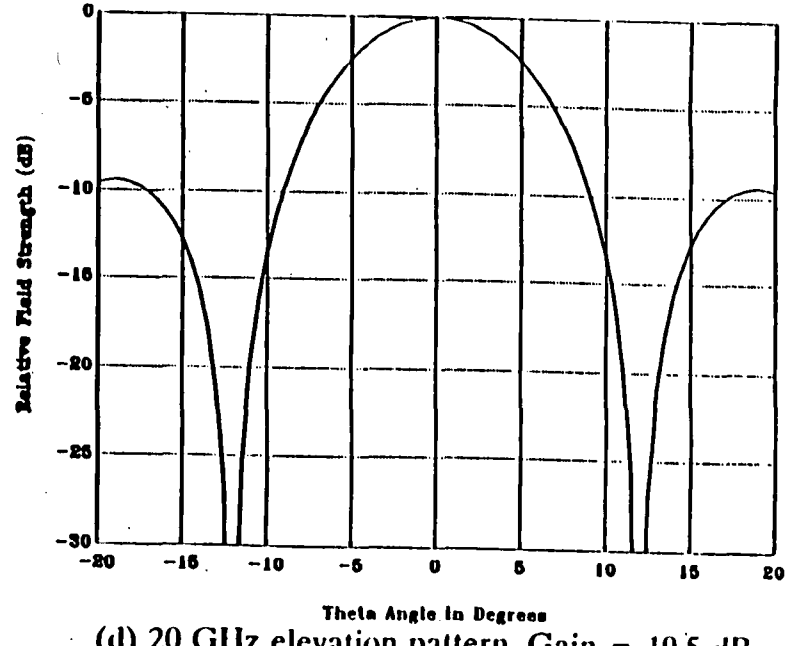

(d) 20 GHz elevation pattern, Gain = 19.5 dB

Figure 13. Typical far-field patterns for a mechanically steered antenna

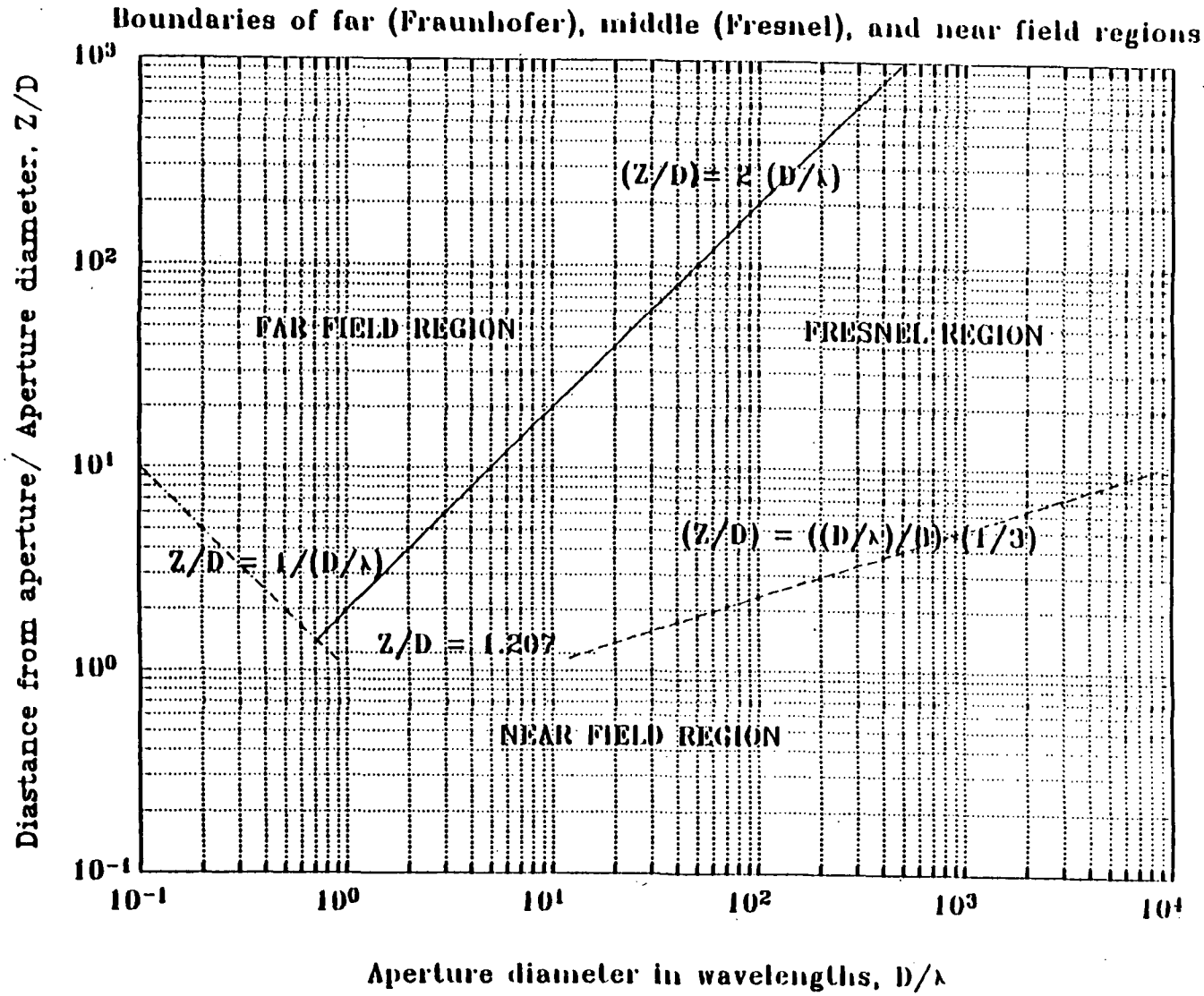

Figure 14. Boundaries of the near, mid(Fresnel), and far (Fraunhofer) field regions of an aperture antenna radiation

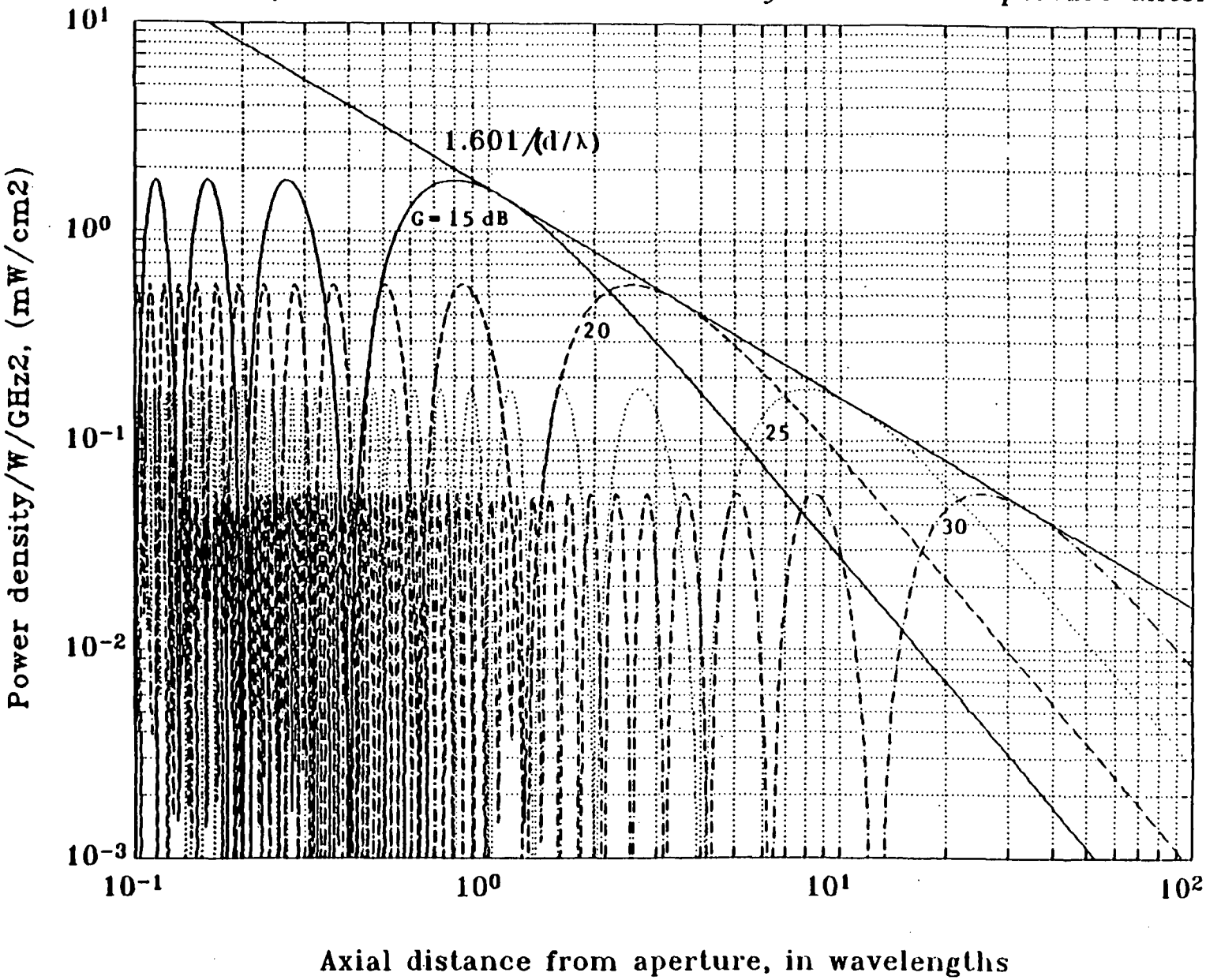

Figure 15. Normalized power density as function of the distance from the aperture for various antenna directivity levels.

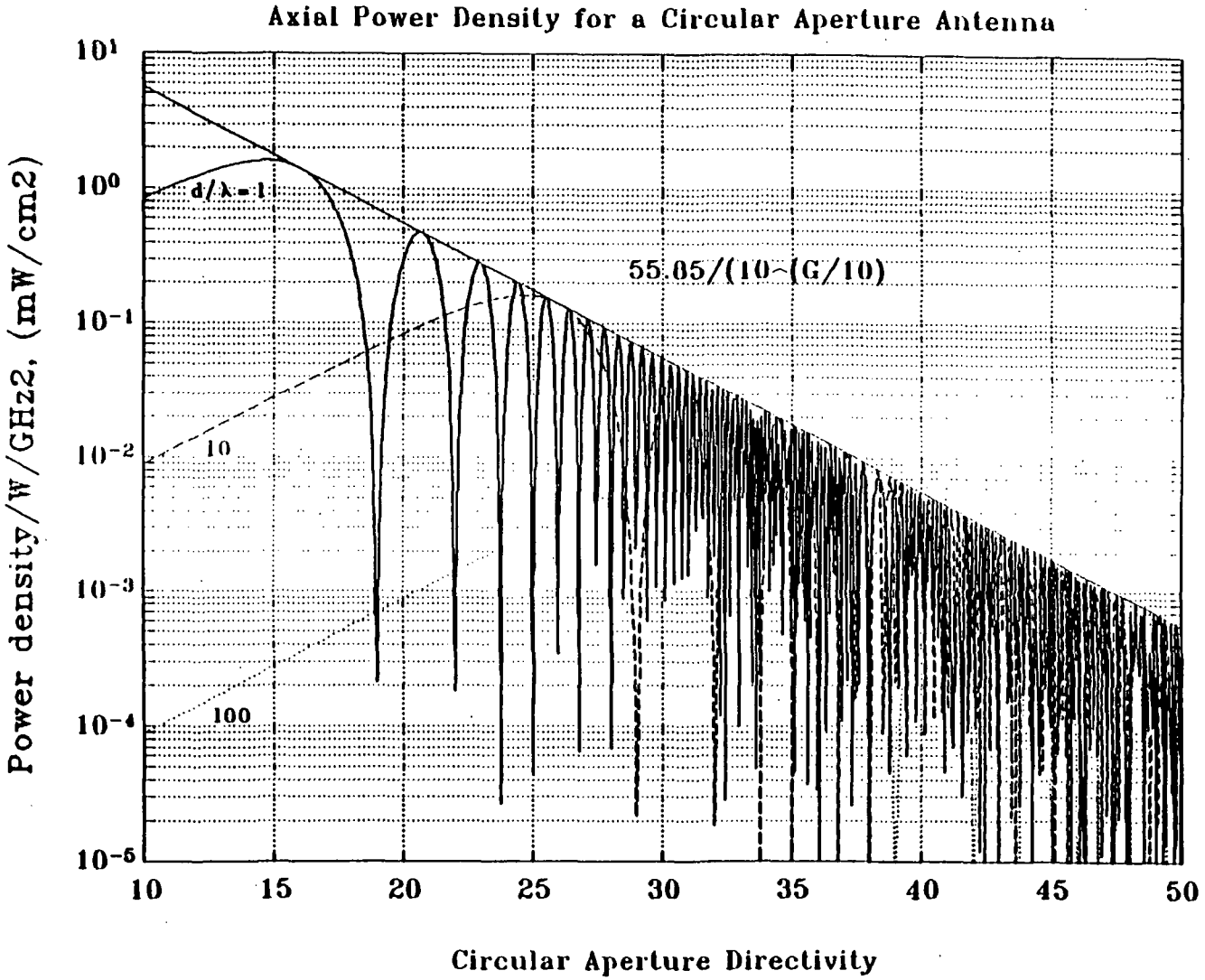

Figure 16. Normalized power density as a function of antenna directivity for various distances from the aperture

APPENDIX I. Gain and figure of merit (G/T) for PASS user terminal antennas (Vahraz Jamnejad)

The performance of the user terminal antennas for Personal Access Satellite System (PASS) can in general be characterized by only two parameters: i) Antenna gain in the transmit mode, ii) Antenna G/T in the receive mode. Indeed, since in principle the antenna may actually utilize two separate radiating apertures or set of radiating elements, different parts of the same aperture, or different subsets of the elements at the two modes of operation, we need to specify only one parameter for each mode of operation.

Thus, the transmit antenna is characterized solely by its gain, G_t and the receive antenna solely by its figure of merit, G_r / T. The concepts of gain and G / T specially when active array antennas are concerned, may not be quite clear and requires some explanation. Here we present a brief description of the gain and figure of merit for receiving antennas. We also take a look at G / T in some typical cases that may occur in actual systems.

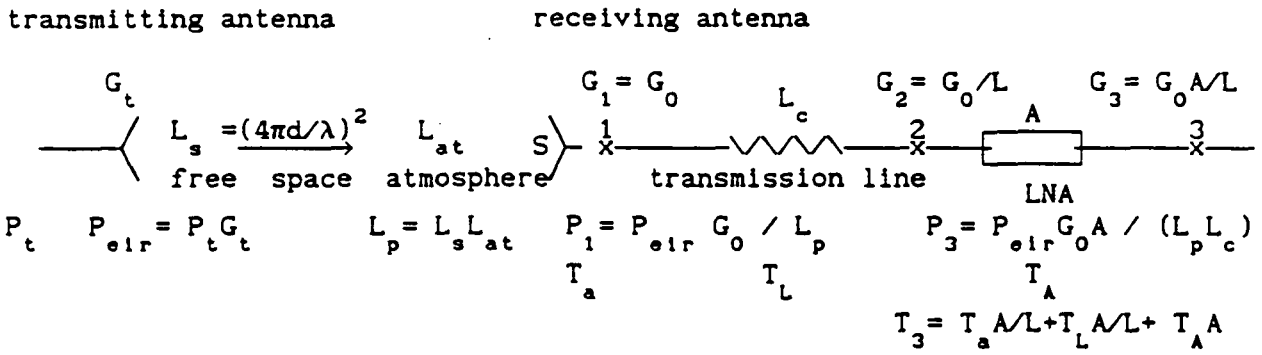

Figure 1. Diagram showing the transmit-receive path

With reference to figure 1, let's define the following parameters:

$G = \eta D = \eta_c G_0$,

$\eta = \eta_c \eta_p$ Beam forming efficiency,

η_p = Polarization efficiency,

η_c = Distribution network(circuit) efficiency,

D = Pattern Directivity,

G_0 = Gain of the antenna directly at the receiving aperture = $\eta_p D$.

Directivity of the antenna, is the ratio of the power density in a

desired direction (usually, the peak direction), to the average power density over the entire space. It includes all the losses associated with forming the antenna beam pattern. For example, we mention the aperture illumination taper and spillover, and surface roughness effects in reflector type antennas, and element tapering loss in arrays. We also include the cross-polarization loss in G_0 which is not usually included in directivity D.

However, we do not include the ohmic losses associated with antenna conducting surfaces, the circuit losses associated with the beam-forming network (such as power dividers and phase shifters), transmission line losses, etc. These losses can be lumped into a single loss figure, here referred to as antenna circuit loss, or beam-forming network efficiency and represented by, η_c, a number smaller than unity. Sometimes circuit loss is represented by the inverse of η_c as

$L_c = 1/\eta_c$ = Circuit Loss Factor (greater than unity).

Here, L_c represents the power lost in the network due to RF absorption and reflection. Strictly speaking, this relation is correct only if the circuit is perfectly matched to the antenna and the receiver, and if the losses are strictly ohmic (in conductors and lossy dielectrics), otherwise it is only an approximation.

Now, for a passive receiving antenna (which does not include any active amplifying elements) the gain, G, is directly measurable at a single physical point, while G_0 is not directly accessible and can only be indirectly deduced, by integration of the theoretically calculated or experimentally measured far field pattern. In an active array antenna where low noise amplifiers are present behind each element or subset of elements, the gain G is not quite meaningful unless one considers the amplifier gain as part of the overall antenna gain. But aperture gain G_0 serves a useful conceptual function in defining the figure of merit, G / T.

The signal power received at the antenna from the spacecraft, directly at input point 1 in Figure 1, is given as:

$$P_1 = \frac{P_t G_t}{4 \pi d^2} S$$

in which,

P_t = spacecraft transmitted power,

G_t = Spacecraft antenna gain,

d = distance from spacecraft to ground antenna, and

S = ground antenna receiving aperture.

Now defining, the Effective Isotropically Radiated Power for the spacecraft transmitting antenna as:

$$P_{eir} = P_t \; G_t,$$

and noting that effective receiving aperture is

$$S = \frac{4\pi}{\lambda^2} \; G_0 \; ,$$

we can rewrite P as:

$$P = \frac{P_{eir}}{(4\pi d/\lambda)^2} \; G_0$$

Defining free space path loss as

$$L_s = (4 \pi d / \lambda)^2,$$

Also representing atmospheric losses by

$$L_a = \text{Atmospheric losses,}$$

we write the total path loss as

$$L_p = L_s + L_a$$

Then The signal power directly at the input to the antenna is

$$P_1 = P_{eir} G_0 / L_p$$

For the arrangement shown in Figure 1, the power at the output of the low noise amplifier (LNA) is given as

$$P_3 = P_{eir} G_0 \; A \; / \; (L_p L_c)$$

The following discussion regarding the noise temperature definitions and calculations are based partially on materials in References [1-3].

The noise temperature directly at the input to the antenna is due to the contributions from space, atmosphere, and ground antenna environment and is dependent on the pattern and directivity of the antenna. It is represented by

$$T_a = \text{Antenna noise temperature}$$

and is in general given by

$$T_a = \frac{1}{4\pi} \iint T_s(\theta,\phi) \; G_0(\theta,\phi) \; \sin(\theta) \; d\theta \; d\phi,$$

in which T_s is the brightness temperature of the discrete or distributed sources in the space around the antenna as function of angle. This integral can be divided over two diffrent regions of space : the upper hemisphere facing the sky (elevation angle $\gamma>0$) and the lower hemisphere facing the ground ($\gamma < 0$). IN the lower half the temperature can be assumed constant and equal to 300° K. In the upper hemisphere this temperature as a function of frequency and for various elevation angles is presented in Figure 2. As can be seen, the temperature in the Ka-band is primarily due to Oxygen and water vapor absorption and peaks at about 20 GHz. Here, we have not considered any localized and/or man-made sources of noise which may be present. The calculation of the above integral is in general requires the actual antenna beam pattern. But in most applications and for relatively narrow beams we can write

$$T_a = \eta_{bl} \times 300 + \eta_{sl} \times T_{sl} + \eta_{ml} \times T_{ml},$$

in which η_{bl} represents the sidelobe efficiency or the percentage of power radiated through the sidelobes. Here by sidelobes we mean all the lobe above the horizon, exclusive of the main beam. Backlobe efficiency refers to the percentage of power radiated below the horizon of the antenna ($\gamma<0$), and finally η_{ml} refers to the percentage of power in the main lobe or beam between the first nulls. T_{sl} and T_{ml} are average temperatures in the main beam and sidelobe directions. For typical directive antennas under consideration we can assume

$$\eta_{ml} \cong 0.8, \ \eta_{sl} \cong 0.1, \ \eta_{bl} \cong 0.1.$$

Consulting Figure 2, the following average temperatures can be assumed at 20 GHz, and for the main beam direction of about 45 degrees above the horizon:

$$T_{ml} \cong T_{bl} \cong 50^\circ \text{ K},$$

The antenna noise temperature is then

$$T_a \cong 0.1 \times 300 + 0.1 \times 50 + 0.8 \times 50 = 75$$

In practice the range of the backlobe with noise temperature of 300 should be extended at least a few degrees above the horizon to account for the hilly terrain, trees and building effects. This may increase the backlobe percentage of power up to 0.2, resulting in the total temperature of

$$T_a \cong 100^\circ \text{ K}$$

The lossy circuit with the loss factor L has a noise temperature which can in general be written as

$$T_L = (F_L - 1) \ T_0$$

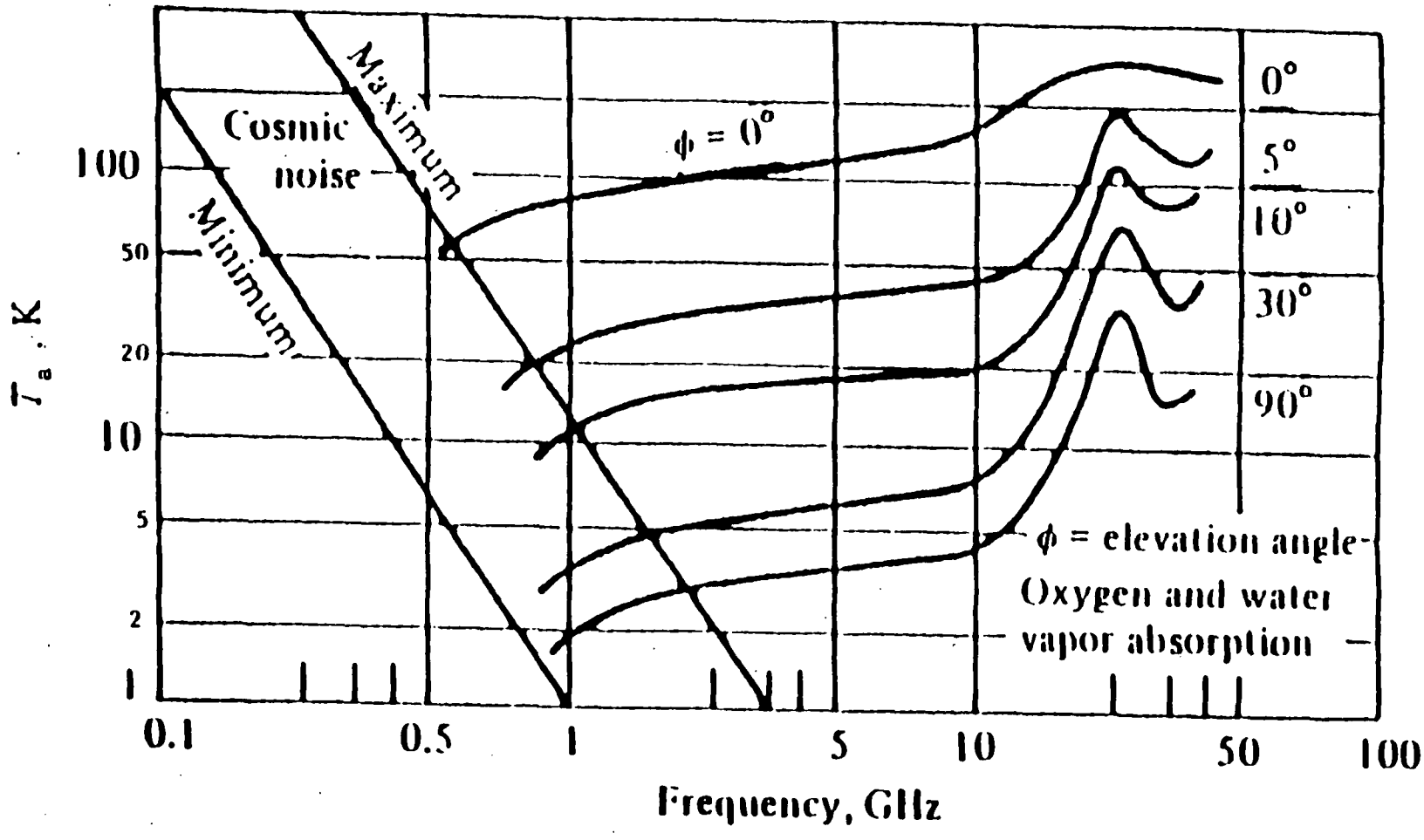

Figure 2. Microwave antenna noise temperature (from Reference 11).

This equation provides a definition for the noise figure F_L. This noise temperature is defined at the input to the lossy circuit.

For a general two-port network as shown in Figure 3, the noise contribution to a load is quite complicated and is given by

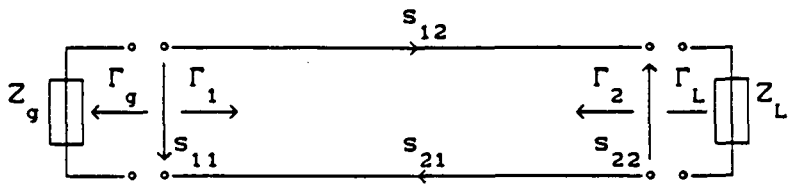

Figure 3. Schematic diagram of a two-port network

$$P_N = \frac{(1-|\Gamma_L|^2)\left\{1-|s_{22}+(s_{21}s_{12}-s_{11}s_{22})\,\Gamma_g|^2-(1-|\Gamma_g|^2)\,|(1-s_{22}\Gamma_L)|^2\,|s_{21}|^2\right\}}{|\,1-s_{11}\,\Gamma_g-s_{22}\,\Gamma_L-(s_{21}s_{12}-s_{11}s_{22})\,\Gamma_g\,\Gamma_L\,|^2}$$

This is in general too complicated to work with. For simplicity we assume this network to be equivalent to a lossy transmission line. Then, the loss for a lossy transmission can in general be given as

$$1 / L = |(1-\Gamma_i\Gamma_o e^{-2\gamma l})|^2\, e^{-2\alpha l},$$

in which Γ_i, and Γ_o are the reflection coefficients towards the input and output sides, γ is the propagation constant, α is the attenuation constant, and l is the line length. for most applications where there is a good match (vswr <2) we can write

$$L \cong e^{2\alpha l}$$

With this approximation, the noise figure is given as

$$F_L = L + (1-M_1)\,(1-1/L)$$

in which M_1 is the mismatch factor at the input junction. It is given by

$$M_1 = \frac{4\,R_l R_r}{|Z_l+Z_r|^2} = 1 - |\Gamma_i|^2,$$

in which Z_l, Z_r, R_l, R_r are impedance and resistance figures to the right and the left of the junction.

The noise figure F_L is ideally under matched conditions ($M_1 = 1$) is

then given as

$$F_L = L$$

In this study an ambient noise temperature of $T_0 = 300^\circ K = 27^\circ C$ is assumed throughout. We think this is a more realistic number than the figure $290^\circ K = 17^\circ C$ used by some in the literature.

The noise temperature of the amplifier is similarly given by

$$T_A = (F_A - 1)\, T_0$$

with

F_A = Amplifier noise figure

Now for a cascaded system with a number of loss and amplification stages as shown in Figure 4, the total noise referenced to the input point is given as

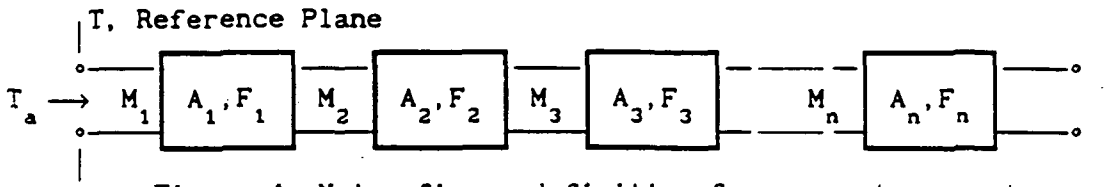

Figure 4. Noise figure definition for an n stage system

$$T = T_a + \frac{(F_1 - 1)}{M_1} T_0 + \frac{(F_2 - 1)}{M_2 (M_1 A_1)} T_0 + \frac{(F_3 - 1)}{M_3 (M_1 A_1 M_2 A_2)} T_0 + \ldots + \frac{(F_n - 1)}{M_n \prod_{i=1}^{n-1} (M_i A_i)}$$

in which F_n is the noise figure of the nth stage, A_n is the amplification or loss at each stage, and M_n is the matching factor at the input to each stage as defined previously.

Now the total noise temperature at point 3 of Figure 1, that is the output of the amplifier, and assuming perfect impedance match throughout, may be written as,

$$T_3 = T_a\, A / L_c + T_L\, A / L_c + T_A A$$

$$= (T_a + T_L + T_A L_c) (A / L_c)$$

In this and following equations we have used L to represent L_c (the circuit loss) for simplicity of notation.

The noise power associated with a temperature T is given by

$$N = K B T$$

K = Boltzman's constant = 1.38×10^{-23} J/ K° = -228.6 dB,
B = receiver bandwidth,
T = total noise temperature at the input to the receiver.

Therefore the carrier power to noise ratio at point 3 of figure 1, i.e., the output of the receiver is given by

$$C / N = (P_{eir} / K B L_s) (G_3 / T_3) = (P_{eir} / K B L_s) (G_1 / T_{31})$$

where $G_1 = G_0$,

and $T_{31} \equiv T$ is the equivalent noise temperature transferred from point 3 to point 1 and given by

$$T_{31} \equiv T = T_a + T_L + T_A L$$

It should be remarked that as long as the final reference point of the G / T specification is fixed the value of this figure of merit calculated at any previous stage remains unchanged. Thus for G/T referenced to the point 3 in Figure 1, we can write

$$G / T\Big|_1 = \frac{G_1}{T_a + T_L + T_A L},$$

$$G / T\Big|_2 = \frac{G_1 / L}{T_a / L + T_L / L + T_A} = \frac{G_1}{T_a + T_L + T_A L}$$

$$G / T\Big|_3 = \frac{G_1 A / L}{T_a A / L + T_L A / L + T_A A} = \frac{G_1}{T_a + T_L + T_A L}$$

However, if the arrangement and location of the amplifier in the system is changed the G/T will change accordingly. To demonstrate this let's consider the following three cases. In all three cases G / T is referenced to point 3.

Case 1) Amplifier after the lossy circuit:

With reference to Figure 5(a), notice that the lossy circuit in this case not only contributes directly to the overall noise temperature, it, in effect, increases the noise contribution of the amplifier. This is consistent with the fact that a lossy circuit stage increases the noise contribution of the later stages.

316

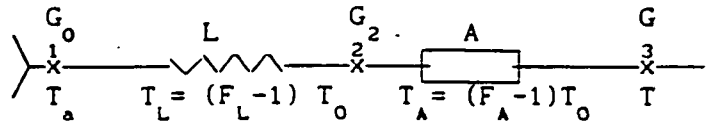

Figure 5(a)

$$G = G_0 \, A / L$$

$$T_3 = T_a A / L + T_L \, A / L + T_A \, A = (T_a + T_L + T_A \, L \,) \, A / L$$

$$G / T = \frac{G_0}{T_a + T_L + T_A \, L}$$

An important fact here is that the power gain of the LNA does not enter this definition. As an example let's assume

$T_a = 100^\circ$, $G_0 = 25\text{dB} \cong 100$,

$L = 5\text{ dB} \cong 3.16$, $F_L = 3.16$,

$A = 20\text{ dB} = 100$, $F_A = 3.5\text{ dB} \cong 2.24$,

Then

$T_L = (3.16-1) \cdot 300 = 648.7$,

$T_A = (2.24-1) \cdot 300 = 371.6$,

$T = 100 + 648.7 + 371.6 \times 3.16 = 1922.9^\circ \cong 32.84$ dB

$G / T = 100 / 1922.9 = 20 - 32.84 = -12.84$ dB

Without the 5 dB network loss the system noise temperature would be

$T = 100 + 371.6 = 471.6 = 26.74$ dB

$G / T = 100 / 472 = 20 - 26.74 = -6.74$ dB

This figure would be even better for an amplifier with lower noise figure. Thus with a no loss BFN and an amplifier noise figure of 2 dB would result in $G / T = -4.4$ dB. Therefore the effect of the network loss on the G / T could be more or less than the loss value in dB, depending on the LNA noise figure. A noisy LNA could completely mask the antenna as well as the network noise temperature effects. While for a good LNA, the network loss could have a very significant effect much larger than its loss value in dB on the overall figure of merit.

Case 2) Amplifier before the lossy circuit:

With reference to Figure 5(b), notice that the contribution of the lossy circuit noise temperature has been reduced by the amplification factor A. This is consistent with the fact that an amplifying stage reduces the noise contribution of the following stages.

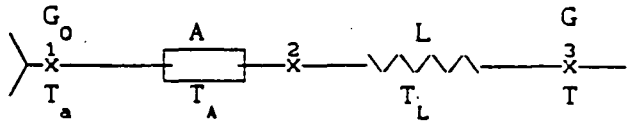

Figure 5(b).

$$G = G_0 \, A / L$$

$$T_3 = T_a \, A / L + T_A \, A / L + T_L / L = (T_a + T_A + T_L / A) \, A / L$$

$$G / T = \frac{G_0}{T_a + T_L / A + T_A}$$

Notice that in this case the power gain of the amplifier does enter the G/T equation. For the example of case 1 we now have:

$T = 100 + 648.7 / 100 + 371.6 = 478.1^{\circ} \cong 26.8$ dB
$G / T = 100 / 478.5 = 20 - 26.8 = -6.8$ dB

As can be seen the G/T is increased by about 3.7. The increase can be higher if the noise figure of the LNA can be further reduced. For example for a noise figure of 2 dB, the G / T is increased to -4.5 dB, a 6 dB improvement compared to the first passive case.

Case 3) Amplifiers before and after the lossy circuit:

With reference to Figure 5(c) which is a compromise case between the previous two cases.

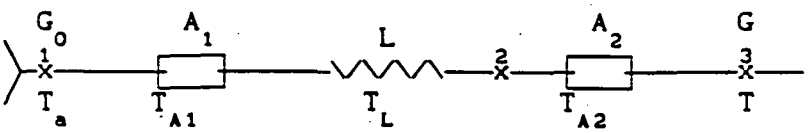

Figure 5(c)

$$G = G_0 \, A_1 A_2 / L$$

$$T_3 = T_a A_1 A_2 / L + T_{A1} A_1 A_2 / L + T_L \, A_2 / L + T_{A2} \, A_2$$

$$= (T_a + T_{A1} + T_L / A_1 + T_{A2} \, L / A_1) \, A_1 A_2 / L$$

$$G / T = \frac{G_0}{T_a + T_{A1} + T_L / A1 + T_{A2} \, L / A1}$$

Now let's consider an example similar to the first case in which the LNA is

218

split into two stages one before and one after the lossy network, each with a 10 dB power gain and a noise figure of 3.5 dB. Then we have,

$T = 100 + 371.6 + 648.7 / 10 + 371.6 \times 3.16 / 10 = 653.9^{\circ} \cong 28.15$ dB
$G / T = 100 / 654.35 = 20 - 28.16 = -8.15$ dB

It is seen that the result falls somewhere in between the previous two cases. The above examples are included in the following table which considers a more general case with two loss and two amplification stages as shown in Figure 6. The relevant formulas are then

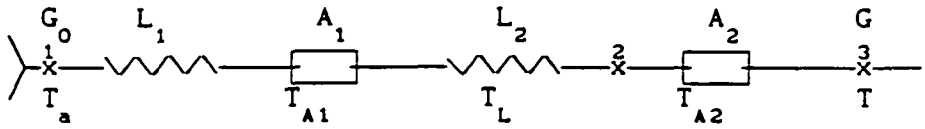

Figure 6

$$G = G_0 A_1 A_2 / (L_1 L_2)$$

$$T_3 = T_a A_1 A_2 / (L_1 L_2) + T_{L1} A_1 A_2 / (L_1 L_2) + T_{A1} A_1 A_2 / L_2 + T_{L2} A_2 / L_2 + T_{A2} A_2$$

$$= (T_a + T_{L1} + T_{A1} L_1 + T_{L2} L_1 / A_1 + T_{A2} L_1 L_2 / A_1) [A_1 A_2 / (L_1 L_2)]$$

$$G / T = \frac{G_0}{T_a + T_{L1} + T_{A1} L_1 + T_{L2} L_1 / A1 + T_{A2} L_1 L_2 / A1)}$$

TABLE 1. SYSTEM NOISE TEMPERATURE AND G/T FOR T= 100° K, G_0= 20 dB

Case	BFN_1 Loss dB	LNA_1 NF, dB	LNA_1 GAIN, DB	BFN_2 Loss dB	LNA_2 NF, dB	LNA_2 GAIN, dB	T, °K	G/T, dB
0a	-	-	-	0	2	20	275.5	-4.4
0b	-	-	-	0	3.5	20	471.6	-6.74
1a	-	-	-	5	2	20	1303.2	-11.15
1b	-	-	-	5	3.5	20	1923.9	-12.84
2a	-	2	20	5	-	-	281.9	-4.5
2b	-	3.5	20	5	-	-	478.1	-6.8
3a	-	2	10	5	2	10	395.8	-5.97
3b	-	3.5	10	5	3.5	10	654.0	-8.15
4a	1	2	20	4	-	-	404.3	-6.07
4b	1	3.5	20	4	-	-	651.2	-8.14
5a	1	2	10	4	2	10	511.2	-7.08
5b	1	3.5	10	4	3.5	10	820.1	-9.14

Based on the cases considered, it is obvious that in antennas with relatively lossy feed distribution networks pre-amplification at the immediate input to the antenna is necessary. This is particularly true in arrays with multiple radiating elements where loss in the distribution network with multiple levels of dividing and combining is quite substantial. The use of amplifiers at the antenna element level as shown in Figures 7(a,b) would then be indeed necessary.

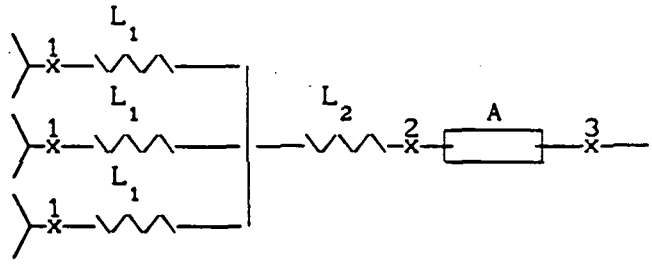

Figure 7(a). Single point amplification in an array

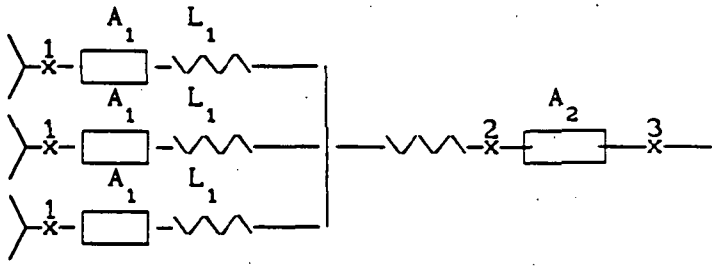

Figure 7(b). Amplification at the radiating element level

REFERENCES

[1] R. E. Collin, *Antennas and Radio Wave Propagation*. Chapter 5.4 McGraw-Hill, 1985.

[2] J. d. Kraus, *Antennas*. Chapter 17. Mcgraw-Hill, 1988.

[3] S. F. Adams, *Microwave Theory and Applications*. Chapter 3. Prentice-Hall, 1969.

330

APPENDIX II
R.F. Radiation Concerns Associated With The PASS User Terminals

P. Cramer

GENERAL PROBLEM

A review was made to determine if the PASS user terminal could present a R.F. radiation safety hazard to users under normal operating conditions. The American National Standards Institute, ANSI, has published the standard ANSI C95.1-1982 [1]. This standard defines the recommended maximum level of RF radiation or electromagnetic fields that would be considered safe for a working environment. This standard was developed under the sponsorship of the IEEE and Naval Electronics Systems Command. The recommendations of this standard were used in evaluating the conditions that need to be met for the safe operation of an user terminal.

Most of the standard is based on the assumption that the user is exposed to an uniform electromagnetic field. This is referred to as whole-body exposure. Figure 1 is a copy of the Radio Frequency Protection Guide for whole-body exposure of human beings from the standard. This guide presents the maximum power density to which an individual can be safely exposed. This guide is based on the assumption that the average specific absorption rate (SAR), the time rate at which electromagnetic energy is coupled to an element of mass of a human body, will not exceed 0.4 W/kg averaged over a 10 minute period. Figure 2 from the standard, contain typical SAR curves for different types of individuals when subjected to a constant power density of 1.0 mW/cm^2 over frequency. The different curves represent measured and empirical cases for individuals ranging in age from infants to adults. The curves shifted to the low frequency end apply to adults and the curves at the highest end apply to infants. Each curve increases rapidly with frequency, reaching a peak and then slowly decreases to a relatively constant level. This variation of energy absorption with frequency is due to the fact that the greatest coupling occurs when the height of an individual exposed to radiation is approximately 0.4 wavelengths and the electric field is oriented along the length of the body. This accounts for the fact that the peak for adults occur at lower frequencies than for infants. The top solid piece-wise curve represents the worst case for a population mix. This curve when normalized to a constant SAR level of 0.4 W/kg, maps approximately into the curve of figure 1 except for the portions of the curve above 1.5 GHz and below 3.0 MHz. These parts of the curve are not allowed to continue to increase, but are held at a constant level and provide an additional safety margin. The time averaged power densities, over a 6 minute period, then must be less than the values in the Radio Frequency Protection Guides of Figure 1. Table 1 is the Protection Guides from the standard in tabular form and also includes levels for the mean squared electric (V^2/m^2) and magnetic (A^2/m^2) field strengths, which are to be used in the near field.

From the Protection Guide, the permissible exposure level at 30 GHz is 5 mW/cm^2. To relate this level to the PASS program, power density patterns were calculated for various sized arrays of patch antenna elements. Patch antenna elements were used since the patch is a strong PASS candidate. 0.3 wavelength wide patches spaced 0.5 wavelengths apart were used. Uniform aperture illumination was assume by assigning the same excitations to each patch element. Five cases ranging from 12 patches to 208 patches were calculated giving a range in gain from 16.4 to 28.4 dB. An input power of 0.1 watt was assume and the antenna dissipative efficiency was 1.0. The transmitter power is equal to the input power divided by the dissipative efficiency. Figure 3, shows the power density calculated along the axis of the antenna. Near the antenna aperture the peak power is not always a maximum on the axis of the antenna as can be seen in Figure 4, which shows the power density pattern in several planes in front of the antenna aperture, the width of the pattern being equal to the size of the antenna aperture. Wherever the off axis level exceeded the on axis level, the level in Figure 3 was corrected to show the maximum off axis level. Therefore, Figure 3 represents the worst case power density in each plane in front of the aperture. For cases where the antenna input power is not 0.1 watt, Figure 3 still can be used by multiplying the power density by the ratio of the desired power to 0.1 watt. The peak or maximum power density for each gain curve varies inversely as the gain, expressed as a power ratio, for gains above 20 dB with an error of less than 6 percent. Therefore, the maximum power density for a given gain can be obtained from Figure 3 by interpolation. For each antenna gain case, it's power density pattern in a plane normal to the antenna axis and at the axial location of it's power density maximum are shown in Figure 5. It can be seen that most of the power lies within one wavelength of the antenna axis. From figure 4, it can be seen that the power density in each plane is lower at a point equivalent to the aperture radius than elsewhere, therefore the maximum or worst case power densities can be considered to be enclosed by a cylinder defined by the antenna perimeter and co-axial with the antenna axis. Figure 6 replots the peak power density points from figure 3, to provide a plot of peak power density as a function of antenna directivity gain.

Of primary interest to the system designer is the effective isotropic radiated power (EIRP). If a program requires a certain EIRP, then the question can be asked, what is the minimum gain antenna that can be used and still meet the safety requirements. Figure 7 is derived from Figure 6 and plots the required gain as a function of EIRP for a power density of 5.0 mW/cm^2. Also included on the same plot is the corresponding input power associated with the indicated gain and the required EIRP.

To get an idea of what restrictions a power density of 5.0 mW/cm^2 might have on the PASS program, consider an antenna gain of 22 dB and an antenna system efficiency of 0.5. From Figure 6, the peak power density is approximately 30.0 mW/cm^2. This would indicate that the 0.1 watt input power would have to be reduced by the ratio of 5/30, or to 0.0167 watts to satisfy the 5.0 mW/cm^2 criteria.

With an efficiency of 0.5, the transmitter power would be 0.033 watts. If an EIRP of 14.0 dBW is required, a transmitter power of 0.32 watts would be needed, which is higher than the allowable 0.033 watts. From Figure 7, however, it can be shown that a gain of 27 dB and a transmitter power of 0.1 watts will satisfy both the EIRP and safety requirements.

ALTERNATE OPTIONS:

The standard recognized that low power devices such as hand-held transceivers where not effectively covered by the standard and therefore provided two "exclusions" for these types of devices. The exclusions were based on the premise that there is a lower likelihood of harm if the exposure is localized such as is the case with the PASS basic user terminals and other handheld transceivers. The first exclusion states that for frequencies between 300 kHz and 100 GHz, the protection guides may be exceeded if the exposure conditions can be demonstrated in laboratory tests to produce specific absorption rates (SAR) below 0.4 W/kg as averaged over the whole body, and spatial peak SAR values below 8 W/kg as averaged over any one gram of tissue. Because of the type of tests specified, it is beyond the scope of this review to take advantage of this exclusion, but could be the basis of a future study. The second exclusion states that for frequencies between 300 kHz and 1 GHz, the protection guides may be exceeded if the total radiated power is seven watts or less. The rationale used to limit the second exclusion to 1 GHz and lower was that antennas at higher frequencies typically had collimated beams, presenting the possibility of exposure to unacceptably high radiation densities. Therefore, the second exclusion does not apply.

The safety standards base their requirements on an average exposure over a 10 minute period of time. This implies that the levels specified in the protection guides can be exceeded as long as the average levels are maintained. It is possible to take advantage of this flexibility if the user terminal radiates power only intermittently. For example, if the user terminal is voice activated, then it is conceivable that the average radiated power would be lower than the instantaneous radiated power. For the 22 dB case, if the instantaneous transmitter power is the proposed 0.32 watts, then the instantaneous aperture power density would be 47.5 mW/cm^2. To meet the protection guide requirements, this would require a 10.5 percent duty cycle over a 10 minute period. Since a hand held terminal is used near or against the head, the question must be raised: are there other hazards to organs such as the eyes if the power density is allowed to increase. This question is address by Om P. Gandhi [2]. He states that in animal experiments, lens opacifications have been noted for power densities greater than 100 mW/cm^2 when applied locally. At lower power densities, he states that no problems have been found and that a chronic far field exposure to 10 mW/cm^2 caused no abnormal ocular changes over a six month period. No safety margins were discussed in relation to the 100 mW/cm^2 test levels, so it is not possible at this point to say that intermittent exposure to 47.5 mW/cm^2 is safe in terms of possible eye damage. It should be pointed out that a safety

margin of at least 10 exists in the values suggested in the protection guide.

If power averaging is considered and it is desired to determine the required antenna gain and input power to provide a given peak or instantaneous EIRP, then additional curves similar to Figure 7 can be derived based on the peak power density to be averaged. However, if a duty cycle of 50 percent is considered giving a maximum power density of 10.0 mW/cm^2, the following approximations can be applied to using Figure 7. First, for a given gain value applied to Figure 7, the corresponding EIRP value read from the figure is increased by 3.0 dB and requires the input power associated with the EIRP value read to be increased by 3.0 dB. Secondly, if a given EIRP value is applied to Figure 7, then the corresponding gain value read from the figure is reduced by 1.6 dB and the corresponding input power is increase by 1.6 dB. This last condition would indicate that for a given EIRP requirement and a 50 percent duty cycle, the required antenna gain could be reduced by 1.6 dB as long as the input power is increased by 1.6 dB. Lastly, if a given input power is applied to Figure 7, then the corresponding EIRP value read from the figure is reduced by 3.3 dB and the gain value associated with the EIRP value read is also reduced by 3.3 dB. These approximations are usable for gains of 20 dB and higher.

From Figure 3, it can be seen that for the lower gain cases, although very high peak power densities result, these peaks are located close to the antenna aperture. The power density then drops off quite rapidly approaching acceptable levels only a short distance in front of the antenna aperture. To take advantage of this fact and to provide protection to a user, a radome could be used to cover the antenna aperture. A radius would have to be selected such that the power density would have reached a safe level by the time the RF fields reach the radome. To get an idea of the size radome that might be needed, the previous example for a 22 dB antenna and an EIRP of 14.0 dBW will be used. An input power of 0.16 watts is required. Using Figure 3, a scale factor of 0.1/0.16 is needed to make it apply to an input power of 0.16 watts. If it is desired to look at the 5.0 mW/cm^2 level, then the 5.0 mW/cm^2 must be multiplied by the scale factor giving a value of 3.1 mW/cm^2. From Figure 3, a 22 dB gain and a level of 3.1 mW/cm^2 corresponds to a distance of approximately 20 wavelengths or at 30 GHz, 20 cm. A radome with a radius this large is not practical, however combined with some of the other techniques discused, a workable design might be provided.

SUMMARY:

A) The most straight forward and safest, if not the most desirable, methods to stay within the safety standards include:

1) The array program was modified to provide the capability to calculate the power density directly on plane surfaces and is available for future calculations. Therefore, each candidate design should be checked for maximum power density to account

for unique properties of each design using the actual element excitations.

2) The standard stated that the mean volts squared per meter squared criteria be used rather than power density in the near field to determine compliance to safety standards. This method was beyond the scope of this review, but should be done with future analysis. A spot check was made and the two approaches appeared to give similar results in the near field. The standard may be recommending the use of the electric field when measuring to determine if a safety hazard exists in the near field rather than as a method of predicting performance.

3) Investigate the feasibility of either increasing the gain of the user terminal antenna or reducing the terminal transmitter power, or both to meet the requirements of the Standard and to satisfy the PASS program requirements.

4) Perform a trade off study of power and gain vs. duty cycle for modest increases in the peak power density above the safe level with the constraint that the average power density does not exceed the safe level.

5) Calculated and plot additional curves similar to Figure 7 for other power densities to support the trade-offs discussed in item 4 above.

6) A trade-off study on the use of radomes should be performed to determine if more favorable designs can be found than the case used as an example in the text above. Also it is recommended that for a given design, sufficient calculations be performed to ensure all unsafe fields are enclosed by the radome

7) Investigate the system, programmatic and technical considerations associated with locating the terminal antenna at a safe distance from the user or other individuals.

B) Approaches requiring more extensive study and development with perhaps less immediate potential might include:

1) Perform a more extensive study of the health safety requirements that would apply to hand held transponders to determine if higher powers can be safely handled. Such studies might include determining what the actual SAR values are to take advantage of the exclusion provisions of the standard, to determine what are safe power density levels for eye exposure and to determine if there are any other limitations to using peak power densities over short periods of time.

2) Investigate and develop techniques: that would constrain the antenna beam from being directed toward the user.

3) Evaluate the use of safety interlocks that would turn off the transmitter power if the unit is not held in a proscribed operating position that has been determine to be safe. An example might be a pressure switch in the ear cup.

References:

[1] ANSI C95.1-1982, "American National Standard Safety Levels with Respect to Human exposure to Radio Frequency Electromagnetic Fields, 300 kHz to 100 GHz", American National Standards Institute, July 30, 1982

[2] Om P. Gandhi, "Biological Effects and Medical Applications of RF Electromagnetic Fields", (Invited Paper), IEEE Trans Microwave Theory and Techniques, Vol. 30, No. 11, November 1982, pp 1831 to 1847.

[3] NIOSH, "Recommendations for a Radiofrequency and Microwave Standard", draft proposal.

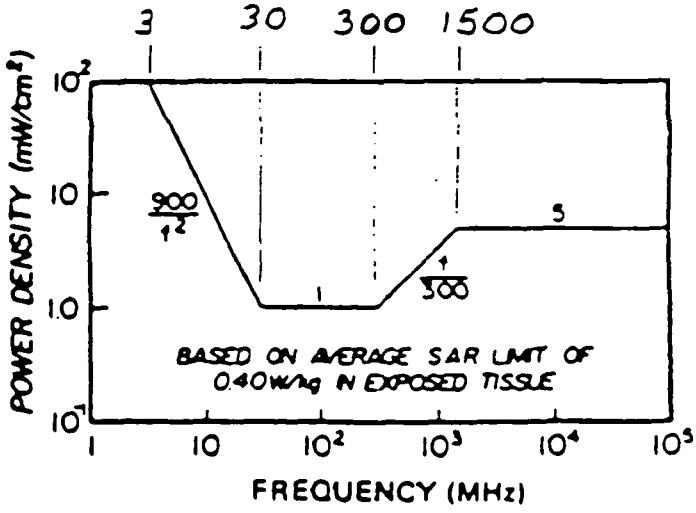

Fig 1
Radio Frequency Protection Guide for Whole-Body Exposure of Human Beings

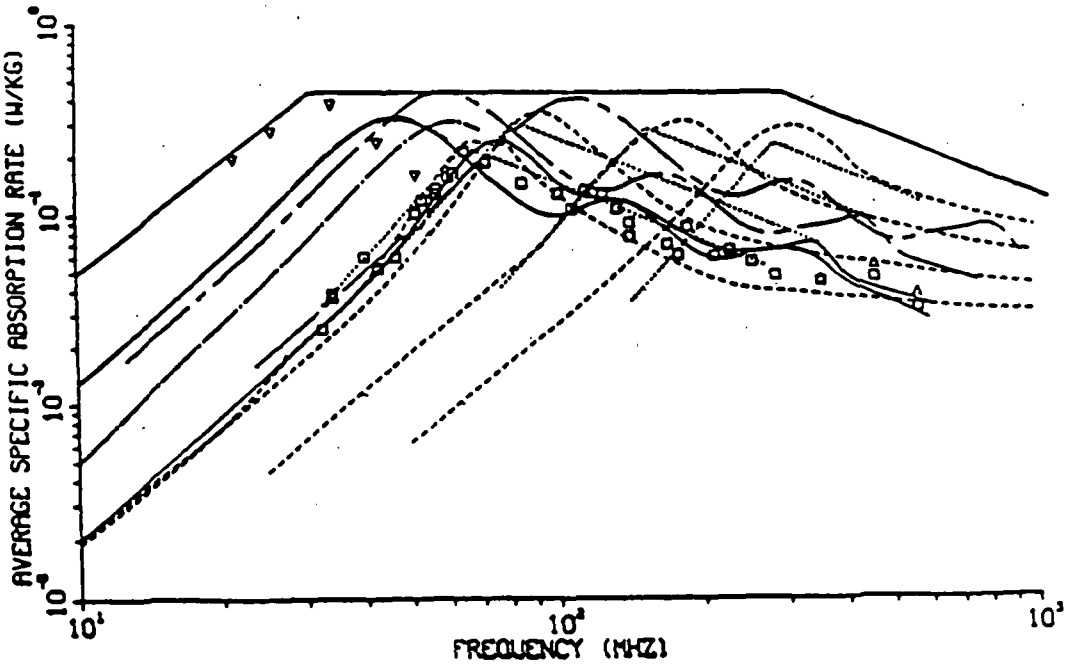

Fig 2

Whole-Body-Averaged SAR

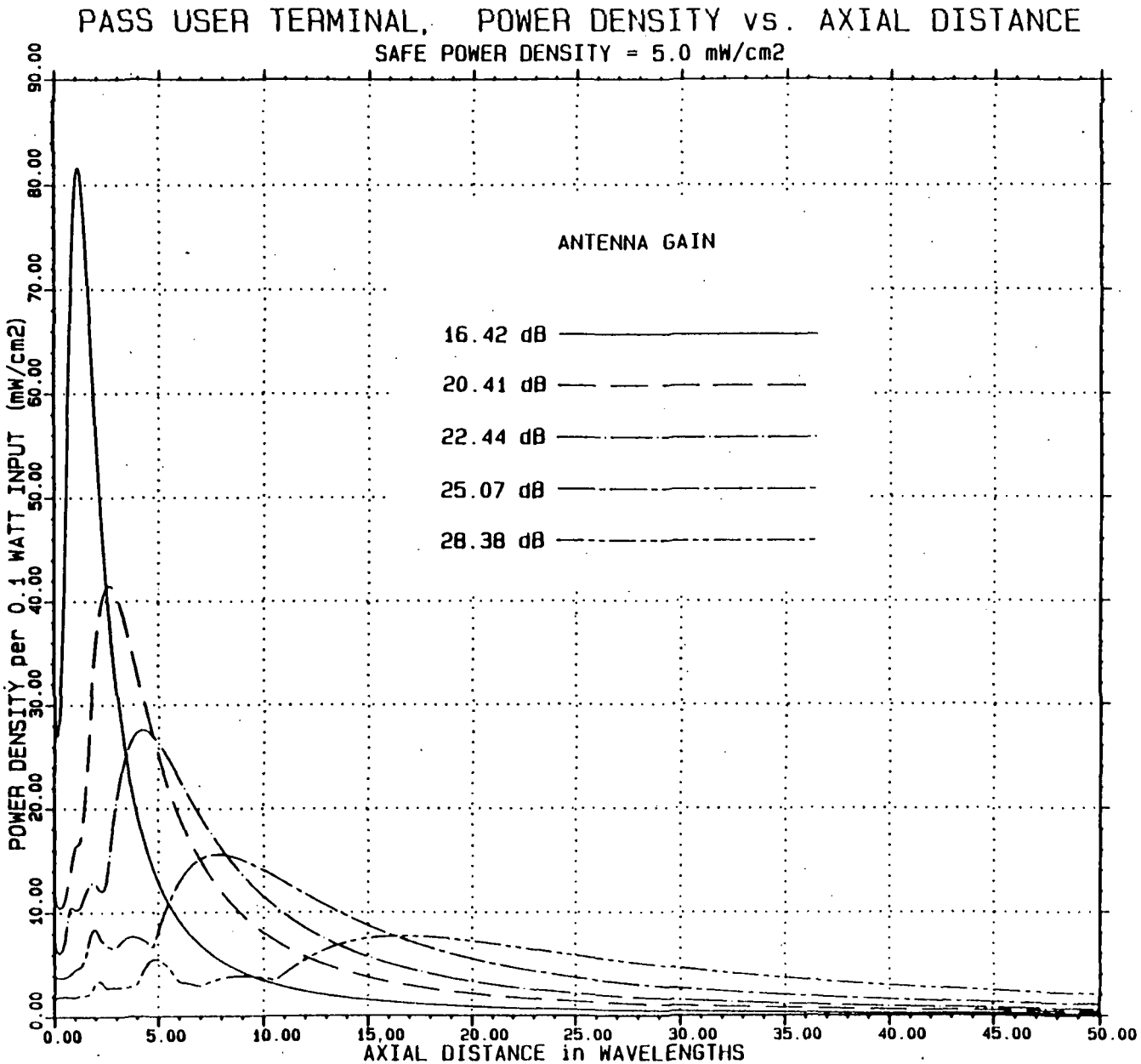
PASS USER TERMINAL, POWER DENSITY vs. AXIAL DISTANCE
SAFE POWER DENSITY = 5.0 mW/cm2
ANTENNA GAIN
16.42 dB
20.41 dB
22.44 dB
25.07 dB
28.38 dB
POWER DENSITY per 0.1 WATT INPUT (mW/cm2)
0.00
10.00
20.00
30.00
40.00
50.00
60.00
70.00
80.00
90.00
0.00
5.00
10.00
15.00
20.00
25.00
30.00
35.00
40.00
45.00
50.00
AXIAL DISTANCE in WAVELENGTHS

Figure 3

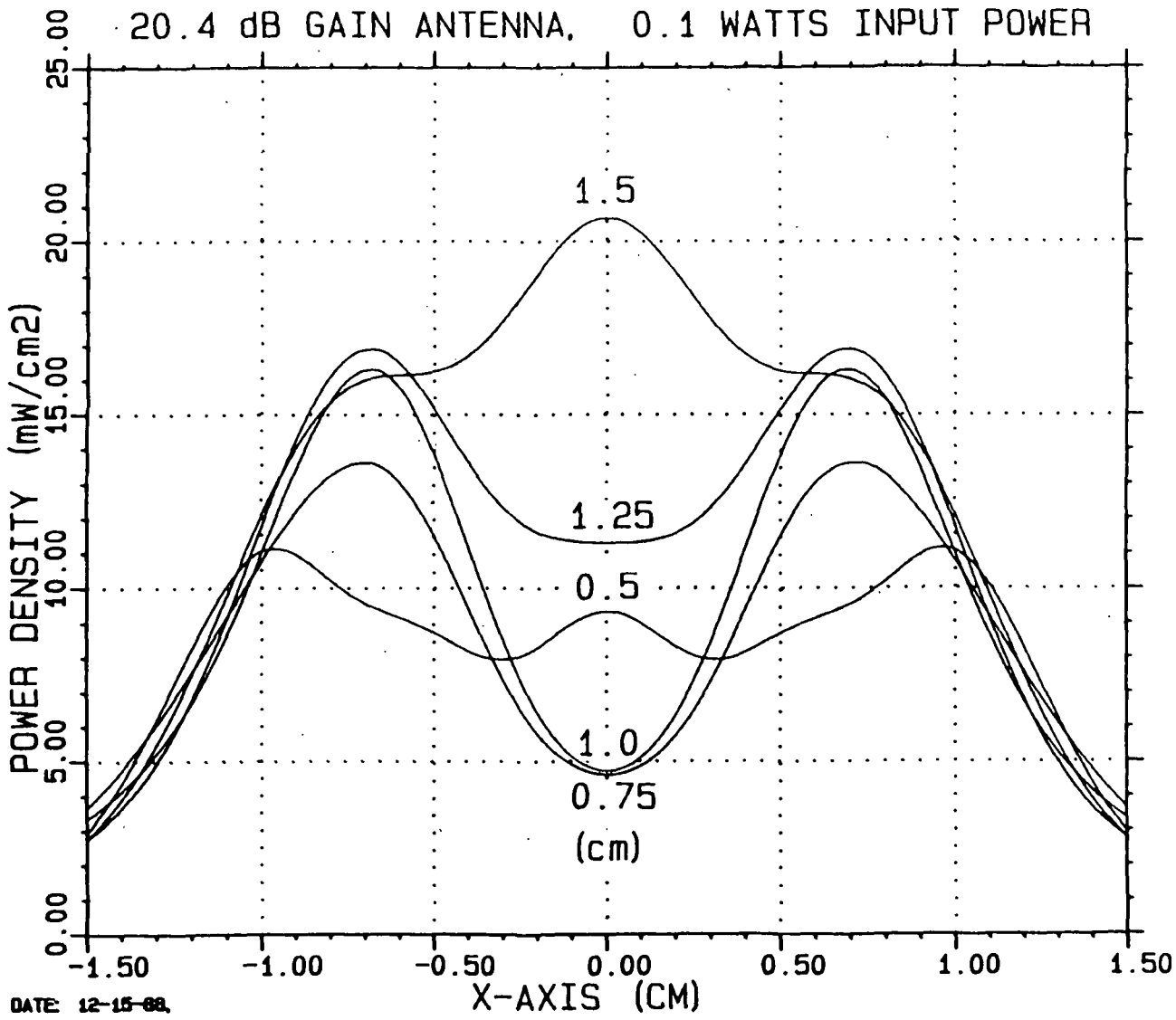
PASS USER TERMINAL, PATTERNS ON PLANE SURFACE
20.4 dB GAIN ANTENNA, 0.1 WATTS INPUT POWER
POWER DENSITY (mW/cm2)
0.00
5.00
10.00
15.00
20.00
25.00
1.5
1.25
0.5
1.0
0.75
(cm)
-1.50
-1.00
-0.50
0.00
0.50
1.00
1.50
X-AXIS (CM)
DATE: 12-15-88

Fig. 4

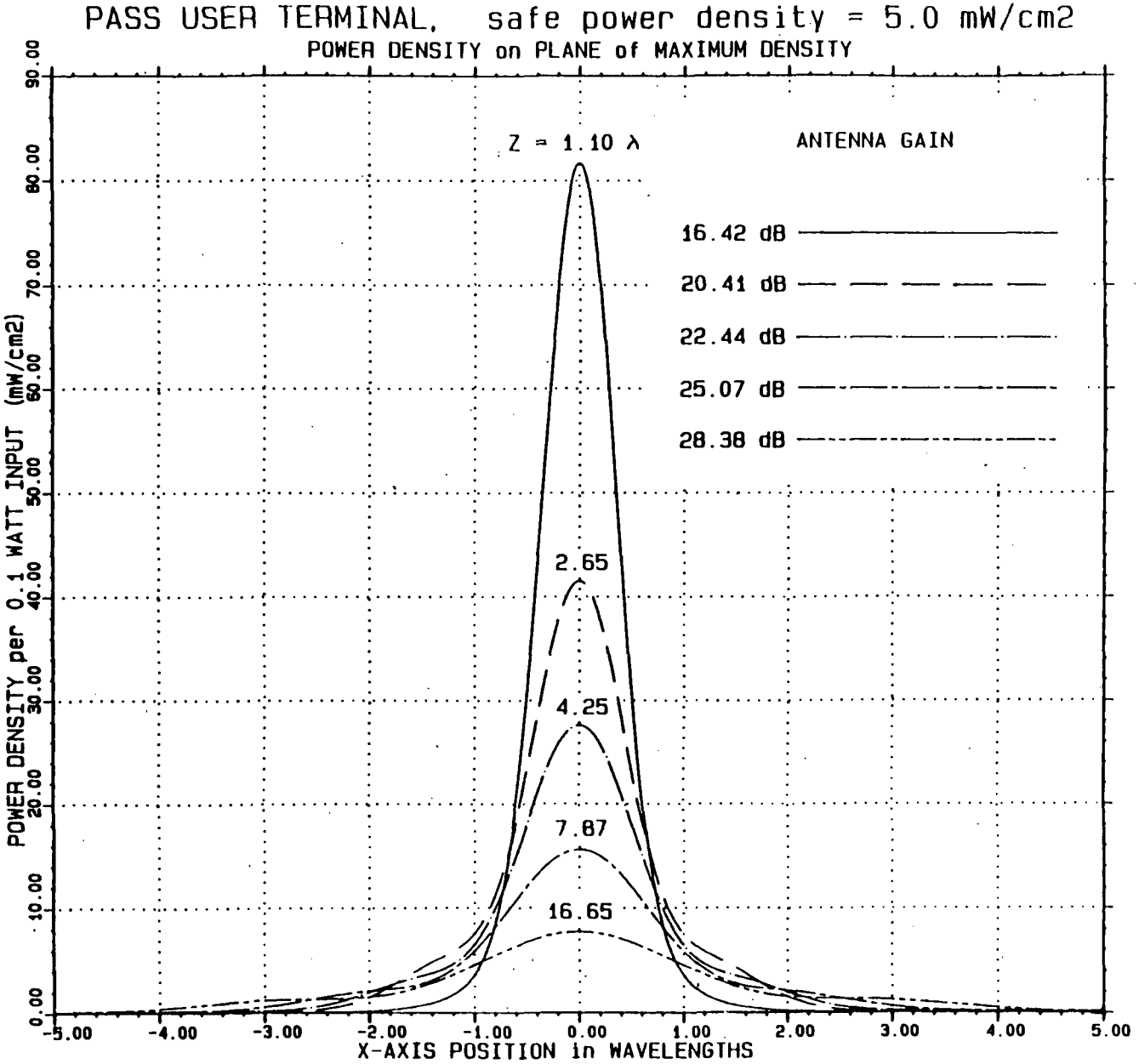
PASS USER TERMINAL, safe power density = 5.0 mW/cm2
POWER DENSITY on PLANE of MAXIMUM DENSITY
Z = 1.10 λ
ANTENNA GAIN
16.42 dB
20.41 dB
22.44 dB
25.07 dB
28.38 dB
2.65
4.25
7.87
16.65
POWER DENSITY per 0.1 WATT INPUT (mW/cm2)
0.00
10.00
20.00
30.00
40.00
50.00
60.00
70.00
80.00
90.00
-5.00
-4.00
-3.00
-2.00
-1.00
0.00
1.00
2.00
3.00
4.00
5.00
X-AXIS POSITION in WAVELENGTHS

Figure 5

PASS USER TERMINAL

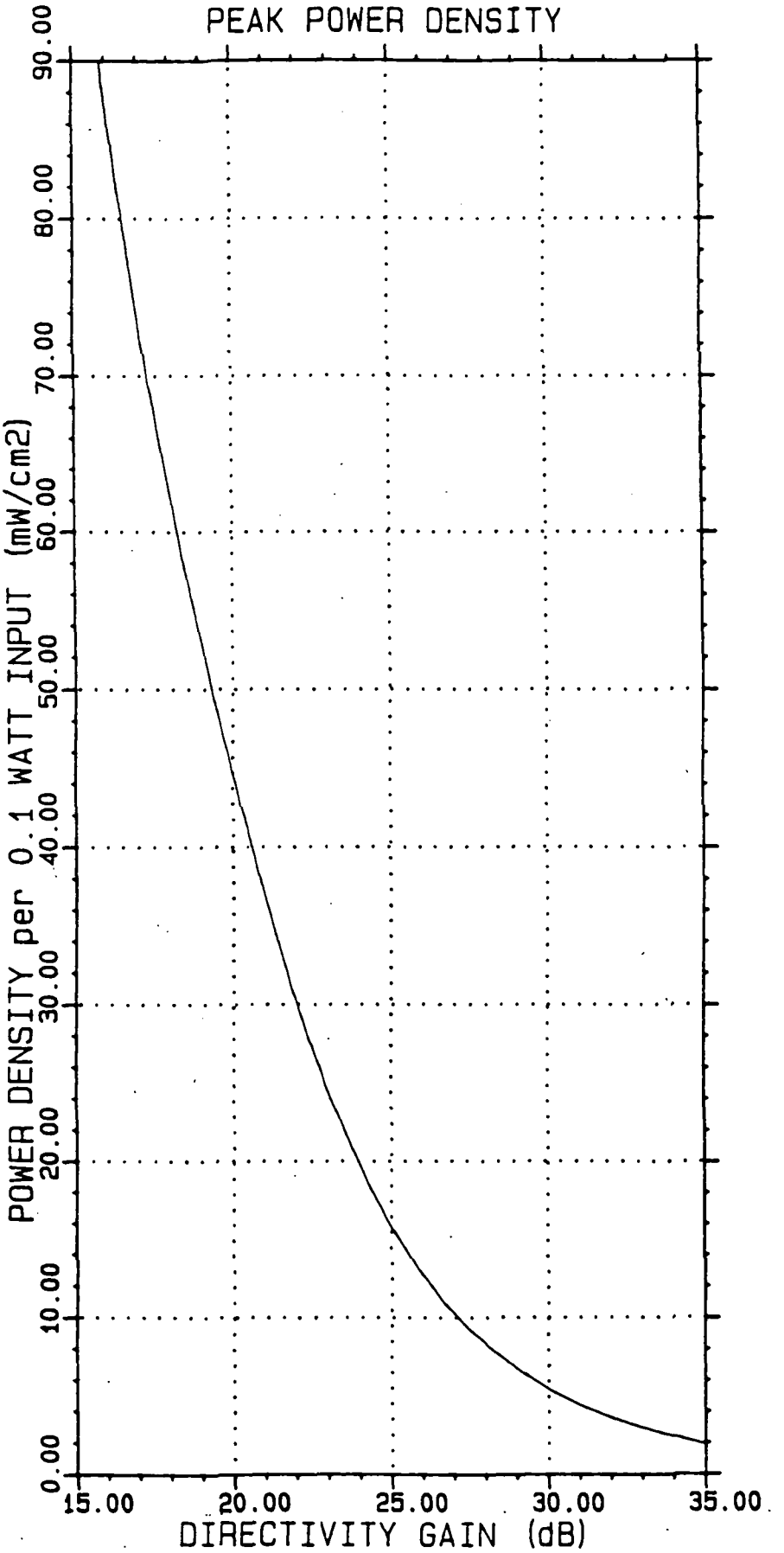

Fig. 6

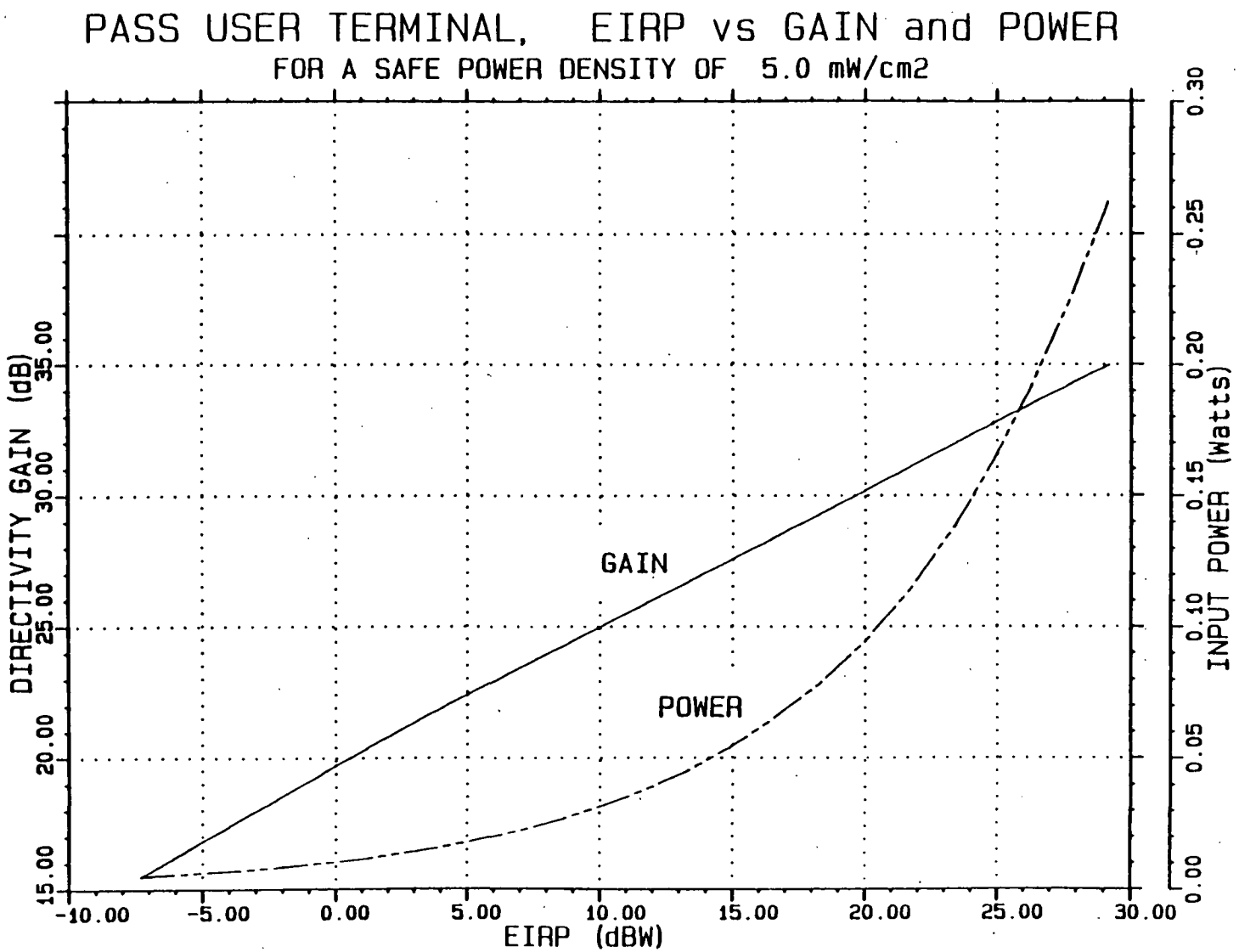
PASS USER TERMINAL, EIRP vs GAIN and POWER
FOR A SAFE POWER DENSITY OF 5.0 mW/cm2
DIRECTIVITY GAIN (dB)
15.00
20.00
25.00
30.00
35.00
INPUT POWER (Watts)
0.00
0.05
0.10
0.15
0.20
0.25
0.30
GAIN
POWER
-10.00
-5.00
0.00
5.00
10.00
15.00
20.00
25.00
30.00
EIRP (dBW)

Figure 7

Radio Frequency Protection Guides

1	2	3	4
Frequency Range (MHz)	E^2 (V^2/m^2)	H^2 (A^2/m^2)	Power Density (mW/cm^2)
0.3 — 3	400 000	2.5	100
3 — 30	4000 ($900/f^2$)	0.025 ($900/f^2$)	$900/f^2$
30 — 300	4000	0.025	1.0
300 — 1500	4000 ($f/300$)	0.025 ($f/300$)	$f/300$
1500 — 100 000	20 000	0.125	5.0

Note: f = frequency (MHz).

Table 1